

SPUTTERED MAGNETITE THIN FILMS ON POLYMER SUBSTRATES FOR
FLEXIBLE SPINTRONICS

MOHAMMAD SHAHNAWAZE ANSARI

UNIVERSITI TEKNOLOGI MALAYSIA

SPUTTERED MAGNETITE THIN FILMS ON POLYMER SUBSTRATES FOR
FLEXIBLE SPINTRONICS

MOHAMMAD SHAHNAWAZE ANSARI

A thesis submitted in fulfilment of the
requirements for the award of the degree of
Doctor of Philosophy

School of Chemical and Energy Engineering
Faculty of Engineering
Universiti Teknologi Malaysia

JULY 2021

DEDICATION

I would like to dedicate this thesis to my beloved son Alhaan, my wife Dr. Sana and my beautiful family for their infinite support and encouragement.

ACKNOWLEDGEMENT

“Learning Today to Teach Tomorrow” Tomorrow is not when you learn. The lesson starts today. Tomorrow teaches where you went wrong yesterday, and you can embrace what went right. It is a part of your past. It is a lesson that grades you. Today is when you learn how to correct where you went wrong yesterday and how to improve upon all you have done correctly in the past.

It is a pleasure to thank those who made this thesis possible. I was in touch with several persons, scholars, educators, and professionals while writing this thesis. They also made a boost to my knowledge and views. In specific, I would like to convey my heartfelt gratitude for support, advice, critique and kindness to my key thesis supervisor, Associate Professor Dr. Mohd Hafiz Dzarfan Othman. He is a wonderful person and I could not have imagined having a better advisor and mentor for my Ph.D study.

I am grateful to Universiti Teknologi Malaysia for providing me International Doctoral Fellowship (IDF), all my colleagues at Advanced Membrane Technology Centre (AMTEC) for their support. My fellow postgraduate students specially Dr. Imran Ullah Khan and Dr. Asim Jilani should also be recognised for their continuous support and timely suggestions. My sincere appreciation also extends to all my colleagues and others who have provided assistance at various occasions.

My sincere respect and affection go out of their blessing, patience and utter love to my cherished family and family in law as well. I acknowledge my sincere indebtedness and gratitude to my father Saleem Mohd and my mother, Rehana Parveen for their love, dream, and sacrifice throughout my life. I acknowledge the sincerity of my parents, who consistently encouraged me throughout my whole educational journey. I am also thankful to my elder brother, Mohd Shahroze Ansari, his wife Dr. Sobia Ansari and their lovely children, Arhab and Aizal for keeping me happy without stress at every step. I want to pay special thanks with lots of love to my younger brother, Ar. Mohd Shahzeb Ansari who is a source of energy for me.

From the bottom of my heart, I would like to say big thank you to a very special person, my wife, Dr. Sana Ansari, who from the start to finish of this research, has provided me continuous motivation and endless assistance. To my precious child, Alhaan, who is a gift of God and my stress buster, may this thesis encourage your future. I am very indebted to Dr. Aslam, Dr. Sumbul and their two beautiful daughters, Aizah and Shiza, who are my inner strength during my PhD.

My study would not have been possible done without the invaluable guidance and help from Dr. Aslam, Dr. Omaish, and Dr. Rajeev from King Abdulaziz University, Jeddah, Saudi Arabia with whom I always feel relaxed which mean a lot to me. Their unwavering support, views, tips, and belief in me are very useful indeed.

ABSTRACT

For flexible and wearable spintronics, it has thus far been a challenge to develop a magnetic material/polymer heterostructure at room temperature due to the thermal sensitivity of polymers. In order to avoid atomic interdiffusion at the interface, reduce deterioration of the films, and prevent the properties of the substrate material from thermal treatment, development of such heterostructures is essential to accomplish at room temperature. Therefore, integration of magnetite (Fe_3O_4) thin films with the polymer substrates to construct a thermally stable flexible spintronic component is of great demand. The primary objective of this research work was to optimize the parameters for room temperature growth of ~ 100 nm thick Fe_3O_4 films through reactive sputtering by flowing oxygen (O_2) and argon (Ar) in the ratio of either 2:20, 3.5:20, or 5:20 sccm on flexible substrates of polycarbonate (PC), polystyrene (PS), polymethyl methacrylate (PMMA), polyvinyl chloride (PVC), and polyethylene terephthalate (PET) developed by drop casting method with a thickness of ~ 250 μm and defect free surfaces. The results showed that the films grown on PC, PMMA, and PET exhibited the pure form of Fe_3O_4 with O_2 flow rate of 3.5 sccm. The Verwey transition (T_v) of ~ 123 K, ~ 124 K, and ~ 126 K; saturation magnetization (M_s) of ~ 220 emu/cm^3 , ~ 235 emu/cm^3 , and ~ 261 emu/cm^3 ; and magnetoresistance (MR) of -7.1% , -7.3% , and -7.8% under $H \parallel \text{Film plane}$ below 60 KOe at 300 K for 100-nm-thick Fe_3O_4 film on PC, PMMA, and PET substrates, respectively were observed. It was found that the antiferromagnetically (AFM) coupled antiphase boundaries (APBs) played a crucial role in these features. Hence, in the second stage of this research work, the finest set of electrical and magnetic properties out of the 50, 100, 200, and 400 nm thick Fe_3O_4 thin films developed on flexible PC with an increase in the deposition time (t_d) from 165 to 1335 s were examined. The maximum value of $M_s \sim 317$ emu/cm^3 and MR -8.3% were obtained for 200 nm thick film for $\text{Fe}_3\text{O}_4/\text{PC}$ heterostructure. However, a T_v of ~ 125 K confirmed the presence of AFM coupled APBs in this architecture, but a negligible loss was observed under flexibility tests *i.e.* resistivity, (M-H and MR under $H(\parallel \text{ and } \perp)\text{Film plane}$ at 300 K) with 90° and 45° of bent angles and cyclability experiments on 100, 200, and 400 bending cycles. Therefore, in the next stage, Fe_3O_4 films with the same thicknesses were grown at room temperature on flexible PMMA substrates as a function of t_d . With a detection of T_v of ~ 127 K which is again a signature effect of APBs, $\text{Fe}_3\text{O}_4/\text{PMMA}$ heterostructure with a film thickness of 200 nm showed an M_s value of ~ 354 emu/cm^3 and MR of -8.6% , larger than the $\text{Fe}_3\text{O}_4/\text{PC}$ heterostructure. Furthermore, the $\text{Fe}_3\text{O}_4/\text{PMMA}$ heterostructure showed $<5\%$ deterioration in the value of M_s and MR under flexibility and cyclability tests. In the final stage of this research work, $\text{Fe}_3\text{O}_4/\text{PET}$ heterostructures with 50 nm to 400 nm of film thickness were developed by the same procedure and the results showed that the T_v for these systems was ~ 122 K which is an indication of almost APB free growth of Fe_3O_4 films on PET. Besides that, M_s of ~ 361 emu/cm^3 , MR of -8.9% , and a negligible loss under different bending tests in comparison to $\text{Fe}_3\text{O}_4/(\text{PC or PMMA})$ heterostructures with the same film thickness proved that $\text{Fe}_3\text{O}_4/\text{PET}$ heterostructure can be a potential candidate for flexible and wearable spintronics.

ABSTRAK

Untuk spintronik boleh lentur dan boleh pakai, terdapat cabaran untuk menghasilkan bahan magnet/heterostruktur polimer pada suhu bilik kerana sensitiviti polimer terhadap haba. Untuk mengelakkan resapan atom di antara muka, kemerosotan filem, dan melindungi sifat-sifat bahan substrat dari rawatan haba, perkembangan heterostruktur pada suhu bilik adalah penting. Oleh itu, integrasi magnetit (Fe_3O_4) filem nipis dengan substrat polimer untuk menghasilkan komponen spintronik boleh lentur yang stabil haba mempunyai permintaan besar. Objektif utama kerja penyelidikan ini adalah untuk mengoptimumkan parameter pertumbuhan suhu bilik filem Fe_3O_4 berketebalan ~ 100 nm melalui teknik percikan reaktif dengan mengalirkan oksigen (O_2) dan argon (Ar) dalam nisbah sama ada 2:20, 3.5:20, atau 5:20 sccm pada substrat polikarbonat (PC) boleh lentur, polistirena (PS), polimetil metakrilat (PMMA), polivinil klorida (PVC), dan polietilena tereftalat (PET) dibangunkan dengan kaedah tuangan titisan dengan ketebalan ~ 250 μm dan permukaan bebas keceleaan. Keputusan menunjukkan filem yang terhasil pada PC, PMMA, dan PET mempamerkan bentuk tulen Fe_3O_4 dengan kadar alir O_2 3.5 sccm. Peralihan Verwey (T_v) ~ 123 K, ~ 124 K, dan ~ 126 K; kemagnetan tepu (M_s) ~ 220 emu/cm^3 , ~ 235 emu/cm^3 , dan ~ 261 emu/cm^3 ; dan rintangan magnet (MR) sebanyak -7.1% , -7.3% , dan -7.8% di bawah satah $\text{H}\parallel\text{Film}$ di bawah 60 KOe pada 300 K untuk filem Fe_3O_4 berketebalan 100 nm masing-masing pada PC, PMMA, dan PET substrat adalah diperhatikan. Didapati bahawa antiferromagnet (AFM) bergandingan sempadan anti fasa (APB) memainkan peranan penting dalam ciri-ciri ini. Oleh itu, pada peringkat kedua kerja penyelidikan ini, set terbaik sifat elektrik dan sifat magnet filem nipis Fe_3O_4 berketebalan 50, 100, 200, dan 400 nm dibangunkan pada PC boleh lentur dengan peningkatan masa pemendapan (t_d) dari 165 hingga 1335 s telah diperiksa. Nilai maksimum M_s ~ 317 emu/cm^3 dan MR -8.3% diperolehi untuk filem berketebalan 200 nm untuk heterostruktur $\text{Fe}_3\text{O}_4/\text{PC}$. Walau bagaimanapun, T_v ~ 125 K mengesahkan kehadiran pasangan AFM dan APBs dalam struktur ini tetapi tidak dijumpai di bawah ujian lenturan iaitu ketahanan, (M-H dan MR di bawah $\text{H}(\parallel\text{dan}\perp)$ satah filem pada 300 K) dengan sudut bengkok 90° dan 45° dan ujian kitaran pada 100, 200, dan 400 kitaran lenturan. Oleh itu, dalam peringkat seterusnya, filem Fe_3O_4 berketebalan yang sama telah dihasilkan pada suhu bilik pada substrat PMMA boleh lentur. Dengan pengesanan T_v ~ 127 K yang merupakan kesan khas APB, $\text{Fe}_3\text{O}_4/\text{PMMA}$ heterostruktur dengan ketebalan filem 200 nm menunjukkan nilai M_s ~ 354 emu/cm^3 dan MR daripada -8.6% , yang mana adalah lebih besar daripada heterostruktur $\text{Fe}_3\text{O}_4/\text{PC}$. Heterostruktur $\text{Fe}_3\text{O}_4/\text{PMMA}$ menunjukkan kemerosotan $<5\%$ dalam nilai M_s dan MR di bawah ujian lenturan dan kitaran. Dalam peringkat akhir, $\text{Fe}_3\text{O}_4/\text{PET}$ heterostruktur dengan ketebalan filem 50 nm hingga 400 nm telah dihasilkan oleh prosedur yang sama dan keputusan menunjukkan bahawa T_v untuk sistem ini adalah ~ 122 K yang merupakan petunjuk pertumbuhan filem Fe_3O_4 pada PET yang hampir bebas APB. M_s ~ 361 emu/cm^3 , MR -8.9% , dan pengabaian di bawah ujian lenturan yang berbeza berbanding dengan heterostruktur $\text{Fe}_3\text{O}_4/(\text{PC}$ atau PMMA) dengan ketebalan filem yang sama membuktikan bahawa heterostruktur $\text{Fe}_3\text{O}_4/\text{PET}$ boleh menjadi calon yang berpotensi sebagai spintronik filem boleh lentur dan boleh dipakai.

TABLE OF CONTENTS

	TITLE	PAGE
	DECLARATION	iii
	DEDICATION	iv
	ACKNOWLEDGEMENT	v
	ABSTRACT	vi
	ABSTRAK	vii
	TABLE OF CONTENTS	viii
	LIST OF TABLES	xiii
	LIST OF FIGURES	xiv
	LIST OF ABBREVIATIONS	xxi
	LIST OF SYMBOLS	xxiii
CHAPTER 1	INTRODUCTION	1
	1.1 Research Background	1
	1.2 Problem Statement	4
	1.3 Objectives	6
	1.4 Scopes	7
	1.5 Research Contribution	10
	1.6 Organization of the Thesis	10
CHAPTER 2	LITERATURE REVIEW	15
	2.1 Introduction	15
	2.2 Advances in Spintronics	17
	2.3 Magnetite as an Emerging Material for Spintronics	20
	2.3.1 Half-Metallic Property	23
	2.3.2 Size Effects and the Thermodynamic Behavior of Magnetite	24
	2.3.3 Spin Accumulation in Fe ₃ O ₄	25
	2.4 Fe ₃ O ₄ Thin Films	27

2.4.1	Crystalline Fe ₃ O ₄ Thin Films with Nanograins	27
2.4.2	Epitaxially Grown Fe ₃ O ₄ Thin Films with Nanometer Thicknesses	28
2.4.3	Growth Techniques	30
2.4.3.1	Pulsed Laser Deposition	30
2.4.3.2	Effect of the Substrate Temperature	30
2.4.3.3	Effect of the Laser Wavelength	32
2.4.3.4	Molecular Beam Epitaxy	34
2.4.3.5	RF Sputtering	38
2.4.3.6	Effect of the Substrate Temperature	39
2.4.3.7	Effect of the RF Power	41
2.4.3.8	Electron-Beam Evaporation	42
2.4.3.9	Ion Beam Deposition	43
2.4.3.10	Electrodeposition	44
2.4.4	The Effect of the Substrate	45
2.4.4.1	Si, MgO and Quartz Substrates	45
2.4.4.2	SrTiO ₃ Substrate	46
2.4.4.3	Al ₂ O ₃ Substrate	50
2.5	Doped Fe ₃ O ₄ Thin Films	54
2.5.1	Co _x (Fe ₃ O ₄) _{1-x} Thin Films	54
2.5.2	Ag _x (Fe ₃ O ₄) _{1-x} Thin Films	55
2.5.3	Zn _x Fe _{3-x} O ₄ Thin Films	56
2.6	Fe ₃ O ₄ -Centered Hybrids	60
2.6.1	Characteristics of Fe ₃ O ₄ -Centered Hybrids	61
2.6.2	Fe ₃ O ₄ -Graphene Hybrids	68
2.6.3	Fe ₃ O ₄ -Transition Metal Dichalcogenides Hybrids	73
2.6.4	Fe ₃ O ₄ -Polymer Hybrids	75
2.6.4.1	Synthesis and Structure of Fe ₃ O ₄ -Polymer Hybrids	75
2.6.4.2	Tunneling Magnetoresistance Effect and Spin Polarization in Fe ₃ O ₄ -Polymer Hybrids	77

2.7	Fe ₃ O ₄ -Centered Flexible Spintronics	80
2.8	Conclusions and Research Gap	85
CHAPTER 3	RESEARCH METHODOLOGY	89
3.1	Research Design	89
3.2	Materials	91
3.3	Drop Casting Method for the Fabrication of Flexible Polymer Substrates	91
3.4	Deposition Technique for Fe ₃ O ₄ Thin Films on Flexible Polymer Substrates	93
3.4.1	RF Sputtering	93
3.5	Surface Analysis and Thickness Measurements of Bare Flexible Substrates	95
3.6	Structural, Morphological and Chemical Characterizations of Thin Films Deposited on Flexible Substrates	95
3.6.1	Crystal Structure and Phase Identification	95
3.6.2	Surface Morphology and Film Thickness	96
3.6.3	Elemental Analysis	98
3.6.4	Crystallographic Structure at Atomic Scale	98
3.6.5	Elemental Composition and Their Chemical States	100
3.7	Electrical and Magnetic Transport Measurements under Normal and Bending Conditions	101
CHAPTER 4	MAGNETITE THIN FILMS GROWN ON DIFFERENT FLEXIBLE POLYMER SUBSTRATES AT ROOM TEMPERATURE: ROLE OF ANTIPHASE BOUNDARIES IN ELECTRICAL AND MAGNETIC PROPERTIES	103
4.1	Introduction	103
4.2	Results and Discussion	104
4.2.1	Flexible Polymer Substrates	104
4.2.1.1	Surface Morphology and Thickness of Polymer Substrates	104
4.2.2	Fe ₃ O ₄ /PC, Fe ₃ O ₄ /PMMA, and Fe ₃ O ₄ /PET Heterostructures at Different O ₂ :Ar Ratio	106

4.2.2.1	Crystal Structure and Phase Identification	106
4.2.2.2	Surface Morphology of Fe ₃ O ₄ Thin Films and Their Thickness	108
4.2.2.3	Crystallographic Structure of Fe ₃ O ₄ Thin Films at Atomic Scale	109
4.2.2.4	Chemical Stoichiometry	110
4.2.2.5	Magnetic Hysteresis Curves	111
4.2.2.6	Magnetoresistance	113
4.2.2.7	Electrical Properties	116
4.3	Conclusions	118
CHAPTER 5	ROOM TEMPERATURE GROWTH OF HALF-METALLIC MAGNETITE THIN FILMS ON POLYCARBONATE WITH DIFFERENT DEPOSITION TIME BY REACTIVE RF SPUTTERING: HETEROSTRUCTURES FOR FLEXIBLE SPINTRONICS	121
5.1	Introduction	121
5.2	Results and Discussion	122
5.2.1	Structural Analysis	122
5.2.2	Electrical and Magnetic Properties	124
5.2.3	Magnetoresistive Properties	128
5.2.4	Electrical and Magnetic Properties under Bending	130
5.3	Conclusions	133
CHAPTER 6	REACTIVELY SPUTTERED HALF-METALLIC MAGNETITE THIN FILMS AT ROOM TEMPERATURE ON POLYMETHYL METHACRYLATE: A PERSPECTIVE FOR FLEXIBLE SPINTRONICS	135
6.1	Introduction	135
6.2	Results and Discussion	136
6.2.1	Structural Properties	136
6.2.2	Electrical and Magnetic Behaviour	140
6.2.3	Magnetoresistance	144

6.2.4	Electrical and magnetic behaviour under bending	146
6.3	Conclusions	150
CHAPTER 7	LARGE SPIN-DEPENDENT TUNNELING MAGNETORESISTANCE IN MAGNETITE/PET HETEROSTRUCTURES DEVELOPED AT ROOM TEMPERATURE: A PROMISING CANDIDATE FOR FLEXIBLE SPINTRONICS	153
7.1	Introduction	153
7.2	Results and Discussion	154
7.2.1	Structural Analysis	154
7.2.2	Electrical and Magnetic Properties	157
7.2.3	Magnetoresistive Properties	162
7.2.4	Magnetic and Electrical Characteristics under Different Bending Conditions	165
7.3	Conclusions	169
CHAPTER 8	CONCLUSIONS AND RECOMMENDATIONS	171
8.1	Conclusions	171
8.1.1	Construction of Flexible Polymer Substrates and the Growth of 100 nm Thick Fe ₃ O ₄ Films on Their Surfaces	171
8.1.2	Development of Fe ₃ O ₄ Thin Films of Various Thicknesses on PC for Flexible Spintronics	172
8.1.3	Growth of Fe ₃ O ₄ /PMMA Heterostructures with Different Film Thicknesses for Bendable/Flexible Spintronics	172
8.1.4	Deposition of Fe ₃ O ₄ Thin Films at RT on PET Substrates for Flexible and Wearable Spintronics	173
8.2	Recommendations for Future Works	174
	REFERENCES	177
	LIST OF PUBLICATIONS	219

LIST OF TABLES

TABLE NO.	TITLE	PAGE
Table 2.1	Expected and measured strain relaxation for Fe ₃ O ₄ films as a result of the thickness.	36
Table 2.2	The effects of substrate on the electrical and magnetic parameters of grown Fe ₃ O ₄ thin films for spintronics.	52
Table 2.3	Selected Fe ₃ O ₄ -based spintronics systems and the effect of different dopants on their electrical and magnetic parameters.	58
Table 2.4	A description of lattice mismatches and the UMA of some manufactured hybrid Fe ₃ O ₄ frameworks.	66
Table 2.5	The magnetic moments of Fe in different graphene-centered systems experimentally tested and estimated in contrast with InAs and GaAs.	69
Table 2.6	Selected polymer substrates for flexible spintronics.	82
Table 3.1	Variation of polymer amount in the solution for the designing of flexible substrates by drop casting method.	91
Table 4.1	Structural, magnetic, and electrical parameters for Fe ₃ O ₄ /PC, Fe ₃ O ₄ /PMMA, and Fe ₃ O ₄ /PET heterostructures with 100 nm of Fe ₃ O ₄ film thickness.	119
Table 5.1	Structural, magnetic, and electrical parameters for Fe ₃ O ₄ /PC heterostructures with different Fe ₃ O ₄ film thicknesses.	133
Table 6.1	Structural, electrical, and magnetic parameters for Fe ₃ O ₄ /PMMA heterostructures with different Fe ₃ O ₄ film thicknesses.	150
Table 7.1	Structural, electrical, and magnetic parameters for Fe ₃ O ₄ /PET heterostructures with different Fe ₃ O ₄ film thicknesses.	169

LIST OF FIGURES

FIGURE NO.	TITLE	PAGE
Figure 1.1	Overall thesis structure.	11
Figure 2.1	Advances in electronics.	15
Figure 2.2	The inverse spinel Fe ₃ O ₄ bulk unit cell, including O (green), tetrahedral Fe (A) atoms (red), and octahedral Fe (B) atoms (yellow).	21
Figure 2.3	Spin polarization (red bars) and T_c (blue triangles) of some designated magnetic materials.	23
Figure 2.4	AFM and M - H curves of iron oxide thin films developed at several T_s : (a and e) 100 °C; (b and f) 300 °C; (c and g) 500 °C; and (d and h) 700 °C.	31
Figure 2.5	(a-c) AFM images, (d-f) M - H curves at different temperatures, and (h-j) M - T curves $H(2 \text{ kOe}) \parallel$ film plane for Fe ₃ O ₄ thin films grown at a T_s of 750 K with a laser wavelength of: (a, d, and h) 213 nm; (b, e, and i) 532 nm; and (c, f, and j) 1064 nm. The inset to (i) shows the calculated value of T_v . (g) The variation of coercivity vs. laser wavelength evaluated at 300, 150, and 100 K.	32
Figure 2.6	RHEED patterns along the $\langle 110 \rangle$ axis and SEM images of 1.7 nm and 7.5 nm thin films deposited through: (a and c) MBE, and (b and d) PLD, respectively. Image in the center of the figure shows the RHEED pattern along the $\langle 110 \rangle$ axis of the substrate (SrTiO ₃ (001)).	34
Figure 2.7	(a-f) AFM images including height profiles and (g-l) M - H curves measured at 10 and 300 K with field-cooled (FC) loops evaluated under an H of 5 kOe at 10 K; (m) variation of resistivity vs. thickness at 300 K; the inset of (m) shows I-V; and (n) resistivity vs. temperature curves for Fe ₃ O ₄ films with various thicknesses in unit cells.	35
Figure 2.8	(a) Observations of thickness vs. O ₂ pressure including phase formation; (b) Fe 2p XPS spectra (for thickness (t) = 20 nm); and (c) M - H curves (t = 20 nm) at 300 K for epitaxially developed iron oxide ultrathin films on MgO(001) under various O ₂ pressures.	37

- Figure 2.9 HRTEM images parallel to the Si(110) zone axis for T_s : (a-b) RT; (c) 250 °C; (d) SAED pattern; (e) XPS spectra for $T_s = 150$ and 400 °C; (f) RT $M-H$ curves for $T_s = 300$ and 400 °C of Si(001)/TiN/Fe₃O₄ (270 nm thick); (g-h) RT $M-H$ curves of 90 nm thick Fe₃O₄ films developed at $T_s = 300$ °C on (g) Si(110) and (h) Si(111). 40
- Figure 2.10 SEM micrographs of Fe₃O₄ crystals developed at -1.15 V for the time interval of: (a) 0; (b) 200; (c) 400; (d) 600; (e) 800; and (f) 1000 seconds; $M-H$ curves under (g) H \parallel buckypaper surface for various t_d and (h) H (\parallel and \perp) buckypaper surface for 800 seconds only. 44
- Figure 2.11 (a) HRTEM overview image; and (b) SAED pattern for the Fe₃O₄/SrTiO₃ interface; SAED simulations along: (c) the $[-110]$ observing plane for both and (d) the $[-110]$ plane for SrTiO₃ and the $[1-10]$ plane for Fe₃O₄; and (e) HAADF STEM image of Fe₃O₄ film and SrTiO₃ substrate along $[-110]$ and $[1-10]$ planes, respectively: Superimposed atomic patterns distinguish the Fe₃O₄ (Fe_B (red), Fe_A (yellow)) and SrTiO₃ (Sr-O (purple), and Ti (green)), respectively); Inset on the right shows two distinct atomic columns ('a' and 'b') for interface region; DFT analysis: (f) Atomic structure across the interface; (g) SDOS for the six structural blocks ($i-vi$). 47
- Figure 2.12 (a) Demonstration of the ST method for Fe₃O₄(001) film development on a SrTiO₃(001) substrate; (b) Temperature vs. time profile of the procedure; (c) $M-H$ curves estimated at 5 K for Fe₃O₄ thin films developed by the standard (400 °C) and ST (1100 °C) techniques. The inset shows the full-scale $M-H$ curves; (d) Variation of M_s and M_r and (e) H_c with T_s . 48
- Figure 2.13 Cross-sectional HRTEM images of the 8 nm thick Fe₃O₄(111) film grown on α -Al₂O₃(0001) at: (a) low; and (b) high magnifications; Resistivity curves for various film thicknesses utilizing a: (c) four-probe and (Inset) two-probe setup; (d) MR measurements at 200 K for different film thicknesses. Inset shows the variation of MR vs. film thickness at $\mu_0 H = 7$ T fitted with a $t^{-1/2}$ reliance. 50
- Figure 2.14 (a) $M-H$ and (b) MT curves of pure and Co-doped Fe₃O₄. 54
- Figure 2.15 (a) MR_{xx} measurements under H \perp film plane at different temperatures for Zn_{0.1}Fe_{2.9}O₄ thin films developed in an Ar environment; (b) RT MR_{xx} curves for various Zn_xFe_{3-x}O₄ films developed in Ar (left) and Ar/O₂-mixture (right) atmospheres; RT $M-H$ curves under H \parallel film plane for Zn_xFe_{3-x}O₄ thin films developed in (c) an Ar environment and (d) an Ar/O₂ (99:1) combination. The insets of (c) and (d) show the M_s and M_r vs. Zn content (x). 56

Figure 2.16	Integrated RT XAS and XMCD spectra of $\text{Fe}_3\text{O}_4/\text{MgO}/\text{GaAs}(001)$ under $H = 4$ T.	62
Figure 2.17	RHEED patterns of: (a) annealed $\text{GaAs}(001)$ substrate; (b) epitaxially grown 6 nm thick Fe film; (c) Fe_3O_4 film obtained via oxidation at 500 K. Suggested arrangements of epitaxial growth: (d) Fe_3O_4 (turned 45°) on (e) $\text{GaAs}(100)$. Insets of (d and e) exhibit key axes for Fe_3O_4 and GaAs , respectively.	64
Figure 2.18	MOKE loops of: (a–p) $\text{Fe}_3\text{O}_4/\text{GaAs}(100)$ and (q–x) $\text{Fe}_3\text{O}_4/\text{MgO}/\text{GaAs}(100)$. The direction of H with regard to the $\text{GaAs}(100)$ substrate is marked on top of every column. The horizontal axis gives the H (-0.7 to $+0.7$ kOe), and the vertical axis provides the MOKE signal.	65
Figure 2.19	Representation of the three possible arrangements of Fe on graphene: top (blue), bridge (green) and hollow (red), and their computed equilibrium distance (d_0) and system free energy (E), referenced to $\text{Fe}^{\text{top}}/\text{graphene}$. The unit cell is displayed as parallelograms (gold color). (b) Spin-resolved band arrangements of a self-supporting Fe ML (left column) and the ML $\text{Fe}^{\text{top}}/\text{graphene}$ (right column), along with their subsequent partial DOSs.	69
Figure 2.20	(a) Atomic modeling of $\text{CoFe}(110)$ on graphene; (b) Estimation of Fermi surfaces of bcc-Co minority-(left) and majority-spin (right) on (110) plane in reciprocal space. The number of Fermi surface sheets is indicated by the color bar. RT sum rule investigations of normalized (c) Fe and (d) Co $L_{2,3}$ -edge XMCD graphs of sintered $\text{CoFeB}/\text{graphene}$.	71
Figure 2.21	Estimated DOSs of Fe and Mo atoms far away from or at the interface, for magnetic contributions of the two Fe_3O_4 layers in: (a,b) parallel or (c,d) anti-parallel arrangements. (e) The atomic composition employed for DOSs computations; (f) TEM image of $\text{Pt}/\text{MoS}_2/\text{Fe}_3\text{O}_4/\text{MgO}$ system; (g-h) MR at different temperatures and R-T curve for the bottom Fe_3O_4 layer (60 nm thick).	74
Figure 2.22	Demonstration of two principal grafting methods: “grafting from” and “grafting to”.	75
Figure 2.23	Structural properties of SiO_2 -coated Fe_3O_4 nanoparticles: (a) Schematic diagram of sonochemical method; TEM images after sonication for (b) 1 and (c) 3 h. Inset of (c) shows HRTEM image of a single core-shell. TEM images of: (d) unmodified; (e) NH_2 -modified; (f) 10; (g) 60; (h) 1000 mg of TEOS in 20 mL of 2-propanol to tune the SiO_2 thickness; and (i) HRTEM image of amorphous SiO_2 -shell-coated Fe_3O_4 core.	76

Figure 2.24	(a) HRTEM of 6 nm Fe ₃ O ₄ nanoparticles sintered at 500 °C for 1 h; (b) SEM image of the device section indicating accumulation of Fe ₃ O ₄ nanoparticles on the SiO ₂ layer and the Pt electrode. Inset of (b) shows a multilayer device. (c) MR curves evaluated at a fixed current of 1 nA at 100 K.	77
Figure 2.25	(a) TEM; (b) HRTEM image of spherical Fe ₃ O ₄ nanoparticles coated with PS; MR curves at 110 K and 280 K for (c) PC and (d) PS coated Fe ₃ O ₄ nanoparticles; Insets (on the left): R vs. T; log R vs. T ^{-1/2} curves; Inset (on the right): I-V graphs at RT; (e) M-H and (f) MR curves in low fields for PS@Fe ₃ O ₄ nanoparticles.	79
Figure 2.26	Structural, electrical, and magnetic properties of Fe ₃ O ₄ /muscovite(mica): (a) Bendable Fe ₃ O ₄ /mica system; (b) Cross-sectional HRTEM with SAED patterns; (c) R-T and M-T curves. Inset shows M-H loops under H (∥ and ⊥) film plane. (d) RT M-H loops under H ∥ film plane; (e) R-T and (f) MR curves at different bending radii. Insets of (e and f) show variation of R and MR values with bending radius and number of bending cycles.	80
Figure 2.27	HAADF-STEM image of: (a) SAO/Fe ₃ O ₄ interface; (b) Fe ₃ O ₄ along [110] plane. Inset of (b) shows flexible PDMS/Fe ₃ O ₄ . Freestanding Fe ₃ O ₄ film under (c-d) bending and (e-f) twisting; M-H loops of PDMS/Fe ₃ O ₄ on bending (R = 4 mm) under (g) H ∥ film plane and (h) H ⊥ film plane; MFM phase mappings of Fe ₃ O ₄ thin film in: (i) flat; (j) bent (R = 4 mm); (k) released conditions; and (l) corresponding histogram.	83
Figure 3.1	Research design flowchart.	90
Figure 3.2	Schematic diagram for the fabrication of flexible PC, PS, PMMA, PVC, and PET substrates by drop casting method.	92
Figure 3.3	Schematic diagram and the growth of Fe ₃ O ₄ thin films on PC, PMMA, and PET substrates through reactive RF sputtering.	94
Figure 3.4	Schematic for principle of XRD (Bragg's law).	96
Figure 3.5	Schematic for working principle of FESEM.	97
Figure 3.6	Schematic for working principle of HRTEM.	99
Figure 3.7	Schematic for working principle of X-ray photoelectron spectroscopy.	100
Figure 3.8	Setup for M-H, MR, and resistivity measurements under various bending conditions.	102

Figure 4.1	Low magnification, high magnification and cross-section images for (a-c) PC, (d-f) PS, (g-i) PMMA, (j-l) PVC, and (m-o) PET.	105
Figure 4.2	XRD spectra of 100-nm-thick Fe ₃ O ₄ thin films on PC, PMMA, and PET substrates using a reactive RF sputtering technique at RT with different O ₂ to Ar ratios.	107
Figure 4.3	Surface morphology and cross-section FESEM images of 100-nm-thick Fe ₃ O ₄ films on (a–b) PC, (c–d) PMMA, and (e–f) PET substrates.	108
Figure 4.4	HRTEM images of 100-nm-thick Fe ₃ O ₄ film on (a) PC, (b) PMMA, and (c) PET substrates, with (d) SAED analysis of the Fe ₃ O ₄ /PET heterostructure.	109
Figure 4.5	XPS bands of the Fe 2p region for (a) Fe ₃ O ₄ /PC, Fe ₃ O ₄ /PMMA, and Fe ₃ O ₄ /PET heterostructures, and (b) Fe ₂ O ₃ /PC formed with O ₂ to Ar ratio of 2 to 20 sccm.	110
Figure 4.6	RT M-H curves for (a) Fe ₃ O ₄ /PC, (b) Fe ₃ O ₄ /PMMA, and (c) Fe ₃ O ₄ /PET heterostructures.	112
Figure 4.7	RT MR curves for (a) Fe ₃ O ₄ /PC, (b) Fe ₃ O ₄ /PMMA, and (c) Fe ₃ O ₄ /PET heterostructures.	115
Figure 4.8	Resistivity as a function of temperature; (a) ρ vs. T plots and (b) $\log(\rho)$ vs. $T^{-1/2}$ plots for the Fe ₃ O ₄ /PC, Fe ₃ O ₄ /PMMA, and Fe ₃ O ₄ /PET heterostructures.	117
Figure 5.1	Structural properties; (a) XRD spectra of reactively sputtered Fe ₃ O ₄ thin films grown on PC substrates at RT, (b-c) and (d-e) Surface morphology and cross-section FESEM images of 50 nm and 400 nm thick Fe ₃ O ₄ films, (f-g) Variation of film thickness vs. t_d and Grain size vs. thickness of the films, (h-i) HRTEM image and SAED patterns for 200 nm thick film, and (j) High-resolution XPS spectra of Fe 2p region.	123
Figure 5.2	Electrical and magnetic properties; (a-b) Parallel and perpendicular M-H curves measured at 300 and 5 K for 200 nm thick Fe ₃ O ₄ film. The insets show enlarged magnetization curves plotted within the range 0 to 10 kOe, (c) Variation of M_s value vs. film thickness, (d) Resistivity as a function of temperature: ρ vs. T plots, and (e) $\log(\rho)$ vs. $T^{-1/2}$ plots for Fe ₃ O ₄ thin films.	125

Figure 5.3	Magnetoresistive properties; (a-b) Parallel and perpendicular MR measurements at 300 K and 5 K for 200 nm thick Fe ₃ O ₄ film. The insets show enlarged MR curves plotted within the range 0 to 10 kOe. (c) Variation of MR vs. film thickness, and (d) Plots of MR vs. M_s at 300 K and 5 K for Fe ₃ O ₄ /PC heterostructures with different thicknesses.	128
Figure 5.4	Electrical and magnetic properties under bending; (a-b) M-H curves with parallel and perpendicular magnetic field, (c) Resistivity vs. temperature, and (d) MR measurements for 200 nm thick Fe ₃ O ₄ film at PC under different bending angles.	131
Figure 5.5	Cyclability test; (a) Resistivity vs. temperature, and (b) MR measurements for 200 nm thick Fe ₃ O ₄ film at PC under different bending cycles.	132
Figure 6.1	(a) XRD spectra of reactively sputtered Fe ₃ O ₄ thin films on PMMA substrates at 300 K, and (b–c) Dependence of film thickness on t_d and variation of grain size vs film thickness	137
Figure 6.2	Morphological and cross-section FESEM micrographs of (a–b) 50 nm thick, (c–d) 100 nm thick, (e–f) 200 nm thick, and (g–h) 400 nm thick Fe ₃ O ₄ film on a PMMA substrate.	138
Figure 6.3	(a) HRTEM image, (b) SAED analysis, and (c) Deconvoluted XPS spectrum for Fe 2p peak of Fe ₃ O ₄ /PMMA heterostructure with 200 nm thickness of Fe ₃ O ₄ film.	139
Figure 6.4	M-H hysteresis loops with H (\parallel and \perp) Film plane at (a) 300 K, (b) 5 K for Fe ₃ O ₄ film of 200 nm thickness. The insets exhibit zoomed M-H curves drawn in the scale of 0 kOe to 10 kOe.	141
Figure 6.5	Deviation of (a) M_s vs film thickness, (b) ρ vs T curves, and (c) Plots of $\log(\rho)$ vs $T^{-1/2}$ for Fe ₃ O ₄ /PMMA heterostructures.	142
Figure 6.6	MR with H (\parallel and \perp) Film plane at (a) 300 K, (b) 5 K for 200 nm thick Fe ₃ O ₄ film. The insets demonstrate zoomed MR curves drawn in the scale of 0 kOe to 10 kOe. (c) Deviation of MR vs thickness of the film.	144
Figure 6.7	M-H hysteresis loops with (a) H \parallel Film plane, and (b) H \perp Film plane for Fe ₃ O ₄ /PMMA heterostructure with a film thickness of 200 nm under various bending conditions	147
Figure 6.8	Deviation of (a) ρ vs T curves, and (b) MR curves for Fe ₃ O ₄ /PMMA heterostructure with a film thickness of 200 nm under various bending angles.	148

Figure 6.9	(a) Plots of resistivity vs temperature, and (b) MR curves for Fe ₃ O ₄ /PMMA heterostructure with a film thickness of 200 nm under various bending cycles.	149
Figure 7.1	Surface morphology and cross-sectional FESEM images of (a–b) 50-nm, (c–d) 100 nm, (e–f) 200 nm, and (g–h) 400 nm thick Fe ₃ O ₄ films on a PET substrate.	155
Figure 7.2	(a) XRD graphs for 50, 100, 200, and 400 nm thick Fe ₃ O ₄ films grown on PET substrates by reactive RF sputtering at RT, (b) Variations in film thickness vs. the t_d , and (c) Grain size vs. film thickness.	156
Figure 7.3	(a) HRTEM image, (b) SAED patterns, and (c) High-resolution XPS spectra of the Fe 2p region of a 200 nm thick Fe ₃ O ₄ film grown on a PET substrate.	156
Figure 7.4	M-H curves recorded at 300 and 5 K for a Fe ₃ O ₄ film with a 200 nm thickness on a PET substrate for the (a) H Film plane, and (b) H⊥Film plane. The insets display the enlarged magnetization curves, plotted within the range of –10 to 10 kOe.	158
Figure 7.5	(a) Variations in the M_s value vs. thickness of Fe ₃ O ₄ film at 300 K and 5 K, (b) Resistivity as a function of temperature (ρ vs. T plots), and (c) $\log(\rho)$ vs. $T^{-1/2}$ plots for Fe ₃ O ₄ /PET heterostructures.	160
Figure 7.6	MR curves; (a-b) H(and ⊥)Film plane at 300 K and 5 K for Fe ₃ O ₄ film of 200 nm thickness. The insets show enlarged MR curves plotted within the range 0 to 10 kOe. (c) Variation of MR vs. film thickness at 300 K and 5 K for Fe ₃ O ₄ /PET heterostructures.	163
Figure 7.7	M-H curves with (a) H Film plane, and (b) H⊥Film plane for 200 nm thick Fe ₃ O ₄ film on PET substrate under various bend angles.	166
Figure 7.8	(a) ρ vs. T plots, and (b) MR curves for 200 nm thick Fe ₃ O ₄ film at PET under different bend angles.	167
Figure 7.9	(a) ρ vs. T plots, and (b) MR measurements for 200 nm thick Fe ₃ O ₄ film at PET under different bending cycles.	168

LIST OF ABBREVIATIONS

2D	-	Two-dimensional
3TH	-	Three-terminal electrical Hanle
APB	-	Antiphase boundary
AC	-	Alternating current
AFM	-	Antiferromagnetism
AMR	-	Anisotropic magnetoresistance
CNF	-	Carbon nanofiber
CVD	-	Chemical vapor deposition
DC	-	Direct current
DFT	-	Density functional theory
DOS	-	Density of state
EDS	-	Energy dispersive X-ray spectroscopy
FC	-	Field cooling
FESEM	-	Field emission scanning electron microscope
FET	-	Field-effect transistor
FIB	-	Focused ion beam
FM	-	Ferromagnetism
FWHM	-	Full width at half-maximum
GMR	-	Giant magnetoresistance
HAADF	-	High-angle annular dark-field
HRTEM	-	High resolution transmission electron microscope
IBD	-	Ion beam deposition
LABE	-	Low angle backscatter electron
MBE	-	Molecular beam epitaxy
MFM	-	Magnetic force microscopy
MOKE	-	Magneto-optical Kerr effect
MOSFET	-	Metal-oxide-semiconductor field-effect transistor
MR	-	Magnetoresistance
MTJ	-	Magnetic tunnel junction
PC	-	Polycarbonate

PDMS	-	Polydimethylsiloxane
PET	-	Polyethylene terephthalate
PLD	-	Pulsed laser deposition
PMMA	-	Polymethyl methacrylate
PPMS	-	Physical properties measurement system
PS	-	Polystyrene
PTFE	-	Polytetrafluoroethylene
PVC	-	Polyvinyl chloride
PVD	-	Physical vapor deposition
RF	-	Radio frequency
RHEED	-	Reflection high-energy electron diffraction
RMS	-	Root mean square
RT	-	Room temperature
SAED	-	Selected area electron diffraction
sccm	-	Standard cubic centimeters per minute
SE	-	Secondary electron
STO	-	Spin torque oscillator
SV	-	Spin valve
TEA	-	Tri-ethanolamine
TEOS	-	Tetraethyl orthosilicate
TFA	-	Trifluoroacetic acid
THF	-	Tetrahydrofuran
TMD	-	Transition-metal dichalcogenide
TMR	-	Tunneling magnetoresistance
UHVC	-	Ultra-high vacuum condition
UMA	-	Uniaxial magnetic anisotropy
vdW	-	van der Waals
VSM	-	Vibrating sample magnetometer
XAS	-	X-ray absorption spectroscopy
XMCD	-	X-ray magnetic circular dichroism
XPS	-	X-ray photoelectron spectroscopy
XRD	-	X-ray diffraction
ZFC	-	Zero-field cooling

LIST OF SYMBOLS

μ	-	Magnetic moment
A	-	Ampere
\AA	-	Angstrom
emu	-	Electromagnetic units
eV	-	Electron Volts
H	-	Magnetic field
H_c	-	Magnetic coercivity
Hz	-	Hertz
J	-	Joule
K	-	Kelvin
M	-	Magnetization
M_r	-	Magnetic retentivity
M_s	-	Saturation magnetization
Oe	-	Oersteds
P	-	Spin polarization
Pa	-	Pascal
R	-	Resistance
t_d	-	Deposition time
T	-	Tesla
T_c	-	Curie temperature
T_s	-	Substrate temperature
T_v	-	Verwey transition
γ	-	Surface tension
λ	-	Wavelength
ρ	-	Resistivity
Ω	-	Ohm

CHAPTER 1

INTRODUCTION

1.1 Research Background

Spin electronics or spintronics is a field which encompasses recognition, management, and utilization of electron spin degree of freedom in solid-state devices to overcome some of the limits set by conventional electronics. It is aspired to get the insight of the interactive connection amongst the spin in addition to its solid-state surroundings and the knowledge obtained helps to fabricate useful devices (Žutić *et al.* 2004). In spintronics, spin of electron rather than its charge is used to transport data for next age of appliances. These novel devices would merge standard micro-electronics and spin-based properties that originate due to the participation amongst carrier spin and the magnetic attributes of the substance (Wolf *et al.* 2001a).

Nowadays, with the ongoing shrinkage of transistor size, electronic devices will inevitably encounter the bottleneck imposed by quantum mechanical effects and they are undergoing shift towards the utilization of electron spin (Powell 2008, Thompson and Parthasarathy 2006). Spintronic devices which rely on electron spin to transmit, process, and store information are more versatile than the silicon-based electronics. Researchers in spintronics field focus on effective polarization of spin and how to read a spin with optimization of coherence length and spin relaxation time in order to assemble commercial spintronic devices.

As one of the most challenging and exciting areas in nanotechnology, spintronics combines the advantages of semiconductors as well as magnetic materials, and spintronic devices are anticipated to be non-volatile, ultra-fast, and energy-saving (Bader and Parkin 2010). Representative spintronic devices, such as spin torque oscillator (STO), MR read head, spin valve (SV) and magnetic tunnel junction (MTJ) are important for science and engineering, since the intriguing electronic, magnetic,

and spin-related properties of these spintronic devices have opened up numerous applications in information storage, computing, communication, sensing, navigation, energy harvesting, and biomedical engineering (Farzad and Alain 2010, Joshi 2016). In 1921, Stern *et al.* (Stern 1921) first measured the spin in a famous experiment whose theoretical explanation was expanded by Kronig *et al.* (Kronig 1926). But, it was in 1925 when the “spin” was principally studied by Uhlenbeck and Goudsmit (Uhlenbeck and Goudsmit 1926). Spin was introduced into quantum mechanics by Pauli in 1927 (Pauli Jr 1927).

Dirac made a momentous contribution to understanding spin by uniting quantum mechanics and special relativity and established a theoretic outline from which the magnetic moment and electron spin were auto tracked. Regardless of the vital character performed by spin of electron in several extents of solid-state physics, it is hardly believed in the conventional field of charge-built electronics. The situation reformed with the finding of oscillatory interlayer switching in Fe|Cr and Co|Cu multilayer by Grünberg *et al.* (Grünberg *et al.* 1986) and soon after by Parkin *et al.* (Parkin *et al.* 1991, Parkin *et al.* 1990, Parkin 1991). This directed to the parallel invention of the giant magnetoresistance (GMR) by dual investigational groups of researchers commanded by A. Fert *et al.* (Baibich *et al.* 1988) and P. Grünberg *et al.* (Binasch *et al.* 1989). The GMR outcome is a breakthrough in solid-state physics for which both the scientists were bestowed the Nobel Prize in Physics (2007) for their contribution. With the curiosity of research and further development of this phenomenon, a fresh subdivision of a condensed matter physics has evolved, that is now known as spintronics or spin-based electronics. In the late '90s, as the spintronic technology continuously thrived, the GMR devices were replaced by tunneling magnetoresistance (TMR) devices (Djayaprawira *et al.* 2005).

Spin-polarized transport takes place if the population of spin (up and down) electrons at the Fermi level are dissimilar. This is normally the case in ferromagnetic metals having alike DOSs for both spin orientations, but the spin states are altered in energy relative to each other causing uneven filling. This imbalance results in magnetic moment and can also influence further properties like variance in the mobility of spin-up and spin-down electrons. There are numerous metals like Fe, Co and Ni with only

one occupied spin band which produce spin-polarized currents up to 40%-50% polarization. However, ideally a 100% spin-polarized current is created; hence there is an intensive research to increase the level of polarization (Prinz 1998). In 2004, a breakthrough was reached with the invention that $\text{La}_{2.3}\text{Sr}_{1.3}\text{MnO}_3$ (LSMO) possesses the capability to produce a spin-polarized current of at least 95% (Bowen *et al.* 2003).

In the thrust of spintronics, functional magnetic materials are very much desired. Particularly, the self-assemblage of multi-component magnetic nanoparticles into precise nanostructures has fascinated huge interests as it offers a promising mode to utilize the spin-dependent effects which arise from interfaces and interaction of the constituent components. Although it is challenging to fabricate controlled assembly of nanocomposite, it is important for development of future spintronic based devices which are built using nanocomposite materials (Jiang *et al.* 2017). To design a semiconducting ferromagnetic flexible substrate for advance spintronics applications, it is necessary that the base matrix polymer should be highly conducting. Therefore, conductive polymer-based nanocomposites are gaining marvelous attention in field of spintronics due to their unique electrical conductivity with other properties such as light weight, easy process ability, flexibility, and favorable environmental stability. This renders them to be utilized in wide potential applications including electronic devices (Cheung *et al.* 2009).

Furthermore, the development of spintronic study has directed to the innovation of a capital of spintronic facts for e.g. TMR (Julliere 1975), the typical (D'yakonov and Perel 1971), contrary (Bakun *et al.* 1984) and quantum (Kane and Mele 2005) spin Hall effects, the spin Seebeck effect (Uchida *et al.* 2008), spin transfer torque (Berger 1996, Slonczewski 1996) and magnonics (Kruglyak *et al.* 2010). Through these inventions, the variety of possible spintronic applications has grown to cover non-volatile and low-power information storage, spin-based logic structures, nanometric oscillators, magnetic cooling, energy harvesting and unique hard disk drive (HDD) recording media (Bader and Parkin 2010).

Flexible electronic structures have earned significant attention over the last decade because of electrifying novel products proposed by subjective external architectures achievable after construction. It is now a subject of focus owing to its mechanical flexibility, low cost and light weight in contrast to rigid material (Melzer *et al.* 2011). Flexible magneto-electronic appliances up to now have mostly been centered on devices using GMR fundamentals within plane magnetized layers and expanding GMR functioning on flexible substrates is of scientific significance (Yuan-fu Chen *et al.* 2008, Melzer *et al.* 2011). Magneto-electronics on bendable substrates permits the absolute incorporation of GMR components on plastic scaffolds, that can be designed into nearly any random structure. Nevertheless, only partial advancement has been made over the last decade on the way to plastic magnetoelectronics attributable to the comparatively insignificant GMR effect attainable on flexible substrates (Yuan-fu Chen *et al.* 2008).

1.2 Problem Statement

It is intricate to incorporate the Fe₃O₄-based devices compatible with flexible polymers substrates. Up till now, Fe₃O₄ thin films were deposited at high temperatures by the physical routes on flexible polymer substrates such as polyimide or Kapton (Vemulkar *et al.* 2016, Wu *et al.* 2016) to get its crystalline form. However, there are enough possibilities of atomic interdiffusion at the interface of the heterostructure, deterioration of the films, and the decay in the mechanical properties of the polymer substrate material at high temperature fabrication.

To tackle such problems, there is a need to grow Fe₃O₄ films at RT and to design other flexible polymer substrates with an optimum thickness which are flexible as well as holding respectable physical and chemical properties to support in the development of flexible spintronic devices. Therefore, in comparison to the other polymers, PC, PS, PMMA, PVC, and PET holds excellent thermal, electrical and mechanical properties which makes them potential candidates for creating flexible substrates within the limit of desired thickness. All these five polymers have melting point above 100 °C, electrical resistivity (PC = 10¹⁴-10¹⁶ Ωcm; PS = 10¹⁸-10²⁰ Ωcm;

PMMA = $>10^{19}$ Ωcm ; PVC = 10^{12} – 10^{15} Ωcm ; PET = $>10^{14}$ Ωcm), Young's modulus (PC = ~ 2 GPa; PS = ~ 3 GPa; PMMA = 2-3 GPa; PVC = 3.4 GPa; PET = 2-4 GPa) and tensile strength (PC = 55-75 MPa; PS = 46-60 MPa; PMMA = 47-79 MPa; PET = 55-75 MPa) etc. additionally, they are cheap, easily available, and effortlessly convertible to the flexible substrates (Bitla and Chu 2017).

To develop defect-free and uniform crystal growth of Fe_3O_4 thin films at RT on the surfaces of these polymers, it is important to design highly flexible PC, PS, PMMA, PVC, and PET substrates having super fine surfaces and holding uncompromised physical properties through drop casting method by varying selected polymer amount in its appropriate solution. The reason behind selecting more than one polymer substrate is to study their effect on the structural, morphological, electrical, magnetic transport and flexible properties of Fe_3O_4 thin films developed on their surfaces at RT. It is expected that the lattice mismatch between the Fe_3O_4 film and different polymer substrates may lead to the residual strain resulting AFM-coupled APBs which may evolve during the growth of Fe_3O_4 thin films and can play a crucial role in the structural, electrical and magnetic transport characteristics of Fe_3O_4 /(PS or PC or PMMA or PVC or PET) heterostructures.

Many PVD techniques such as reactive RF sputtering, MBE, e-beam evaporation, and IBD have been employed for the deposition of Fe_3O_4 nanostructures at RT on different substrates for e.g. Si (Hong *et al.* 2003, Jain *et al.* 2004, ZL Lu *et al.* 2007, Park *et al.* 2005a), glass and Kapton (Furubayashi 2003, Hui Liu *et al.* 2003a, Hui Liu *et al.* 2003b, Liu *et al.* 2004b), $\alpha\text{-Al}_2\text{O}_3(0001)$ (Xiangbo Liu *et al.* 2014b) and MgO (Lai *et al.* 2004). Out of these techniques, reactive RF sputtering is the most versatile method which allows to use numerous combinations of O_2 vs. Ar ratios to develop polycrystalline Fe_3O_4 nanostructures in the form of good quality thin films with homogenous surface and uniform thickness. The reason behind applying different O_2 flow rate with respect to Ar is to achieve single phase Fe_3O_4 thin films. The reactively sputtered Fe_3O_4 thin films may adulterate with the Fe metallic phase if the O_2 flow rate is low, conversely, get contaminated with $\alpha\text{-Fe}_2\text{O}_3$ if the O_2 flow rate is high due to excess amount of O_2 species available to oxidize Fe atoms during the growth at RT. However, to the best of our knowledge, nobody has used this technique

for the growth of Fe_3O_4 thin films on flexible PC, PS, PMMA, PVC, and PET substrates at RT.

In this research work, one more growth parameter known as deposition time (t_d) will also be varied to get various thicknesses of Fe_3O_4 films on flexible PC, PS, PMMA, PVC, and PET substrates at RT through reactive sputtering technique by applying optimum $\text{O}_2:\text{Ar}$ ratio. The reason behind developing $\text{Fe}_3\text{O}_4/(\text{PS}$ or PC or PMMA or PVC or $\text{PET})$ heterostructures with different film thickness is to find out its effect on the structural, electrical, magnetic transport, and bending properties of these systems. On the basis of the results, it will be concluded that which particular heterostructure (Fe_3O_4 film with a specific thickness on PS or PC or PMMA or PVC or PET substrate) is holding the finest set of features with least influence of AFM coupled APBs essential for the application of flexible and wearable spintronics.

1.3 Objectives

The main goal of this research work is focused on flexible and wearable spintronics by means of developing Fe_3O_4 thin films of various thicknesses on selected polymer substrates at RT to avoid atomic interdiffusion at the interface, to reduce deterioration of the films, and to prevent the mechanical properties of the substrate material from thermal treatment. Our efforts have a potential to innovate a decisive move in the direction of Fe_3O_4 -centred flexible spintronics and can offer a new platform for technological applications.

The objectives of the research are:

- (a) To study the effect of polymer amount in the solution on the morphology and thickness of PC, PS, PMMA, PVC, and PET flexible substrates and to grow Fe_3O_4 thin films on their surfaces using reactive sputtering at RT by varying O_2 flowrate.

- (b) To investigate the influence of PC substrate and the t_d of Fe_3O_4 thin films on the morphology, chemical stoichiometry, electrical and magnetic transport characteristics under various bending conditions for $\text{Fe}_3\text{O}_4/\text{PC}$ heterostructures.
- (c) To examine the effect of PMMA substrate and Fe_3O_4 film thicknesses as a function of t_d on the structural, electrical and magnetic transport properties for $\text{Fe}_3\text{O}_4/\text{PMMA}$ heterostructures under various bending conditions.
- (d) To evaluate the influence of PET substrate and t_d of Fe_3O_4 thin films on the morphology, film thickness, chemical stoichiometry, electrical and magnetic transport under various bending conditions for $\text{Fe}_3\text{O}_4/\text{PET}$ heterostructures.

1.4 Scopes

In order to achieve the objectives, four scopes have been identified in this research. The scopes are:

- (a) Designing flexible polymer substrates of PC, PS, PMMA, PVC, and PET by drop casting method and to develop Fe_3O_4 thin films on their surfaces through reactive RF sputtering technique at RT by varying O_2 flowrate.
 1. The amount of polymer in the solution was varied from 0.75, 1, and 1.25 g to achieve 250 μm thickness of the polymer substrates.
 2. Investigating their surface morphology and thickness through field emission scanning electron microscope (FESEM).
 3. Producing Fe_3O_4 thin films on flexible by reactive RF sputtering technique at RT by flowing O_2 and Ar together in the ratios of 2:20, 3.5:20, and 5:20 sccm, respectively.
 4. Phase confirmation and crystal structure Fe_3O_4 thin films grown on different flexible polymer substrates by using X-ray diffraction (XRD).

5. Morphology, thickness of the film, atomic arrangement, crystallographic patterns, and chemical stoichiometry by using FESEM, energy-dispersive X-ray spectroscopy (EDS), high-resolution transmission electron microscope (HRTEM), selected area electron diffraction (SAED) and X-ray photoelectron spectroscopy (XPS).
 6. M-H and MR curves at 300 K and 5 K under H(\parallel and \perp)Film plane by using physical properties measurement system (PPMS).
 7. Resistivity measurements between the range of 300 K to 50 K by using PPMS.
- (b) Growing Fe₃O₄ thin films on flexible PC substrates with various t_d (~165, 335, 665, and 1335 seconds) at RT by reactive RF sputtering technique and characterizing these Fe₃O₄/PC heterostructures in terms of their structural, electrical and magnetic properties.
1. Phase confirmation and crystal structure by using XRD.
 2. Morphology, thickness of the film, atomic arrangement, crystallographic patterns, and chemical stoichiometry by using FESEM, EDS, HRTEM, SAED and XPS.
 3. M-H and MR curves at 300 K and 5 K under H(\parallel and \perp)Film plane by using PPMS.
 4. Resistivity measurements between the range of 300 K to 50 K by using PPMS.
 5. M-H under H(\parallel and \perp)Film plane, MR curves under H \parallel Film plane at 300 K and resistivity (300 K to 50 K) with different bending angles (unbent, 90°, 45°, and released) and bending cycles (1, 100, 200, and 400) by using PPMS.

- (c) Developing Fe₃O₄ thin films on flexible PMMA substrates with various t_d (~165, 335, 665, and 1335 seconds) at RT by reactive RF sputtering technique and characterizing these Fe₃O₄/PMMA heterostructures in terms of their structural, electrical and magnetic properties.
1. Phase confirmation and crystal structure by using XRD.
 2. Morphology, thickness of the film, atomic arrangement, crystallographic patterns, and chemical stoichiometry by using FESEM, EDS, HRTEM, SAED and XPS.
 3. M-H and MR curves at 300 K and 5 K under H(\parallel and \perp)Film plane by using PPMS.
 4. Resistivity measurements between the range of 300 K to 50 K by using PPMS.
 5. M-H under H(\parallel and \perp)Film plane, MR curves under H \parallel Film plane at 300 K and resistivity (300 K to 50 K) with different bending angles (unbent, 90°, 45°, and released) and bending cycles (1, 100, 200, and 400) by using PPMS.
- (d) Producing Fe₃O₄ thin films on flexible PET substrates with various t_d (~165, 335, 665, and 1335 seconds) at RT by reactive RF sputtering technique and characterizing these Fe₃O₄/PET heterostructures in terms of their structural, electrical and magnetic properties.
1. Phase confirmation and crystal structure by using XRD.
 2. Morphology, thickness of the film, atomic arrangement, crystallographic patterns, and chemical stoichiometry by using FESEM, EDS, HRTEM, SAED and XPS.
 3. M-H and MR curves at 300 K and 5 K under H(\parallel and \perp)Film plane by using PPMS.
 4. Resistivity measurements between the range of 300 K to 50 K by using PPMS.

5. M-H under H(\parallel and \perp)Film plane, MR curves under H \parallel Film plane at 300 K and resistivity (300 K to 50 K) with different bending angles (unbent, 90°, 45°, and released) and bending cycles (1, 100, 200, and 400) by using PPMS.

1.5 Research Contribution

This study could be beneficial to the researchers in the field of flexible spintronics regarding to the knowledge generation on fabrication of different types of flexible substrates followed by thin film deposition of Fe₃O₄ thin films by physical route. In addition, it would also lead to the development of low-cost flexible spintronics devices that would be able to compete economically with conventional spin-based electronic devices.

1.6 Organization of the Thesis

This thesis is divided into eight chapters including the preparation of highly flexible polymers in the form of free-standing substrates for the growth of Fe₃O₄ thin films, the evaluation of the fabrication process and the factors affecting the process, the examination of different heterostructures and their performances for flexible and wearable spintronics. Figure 1.1 depicts the overall structure of the thesis.

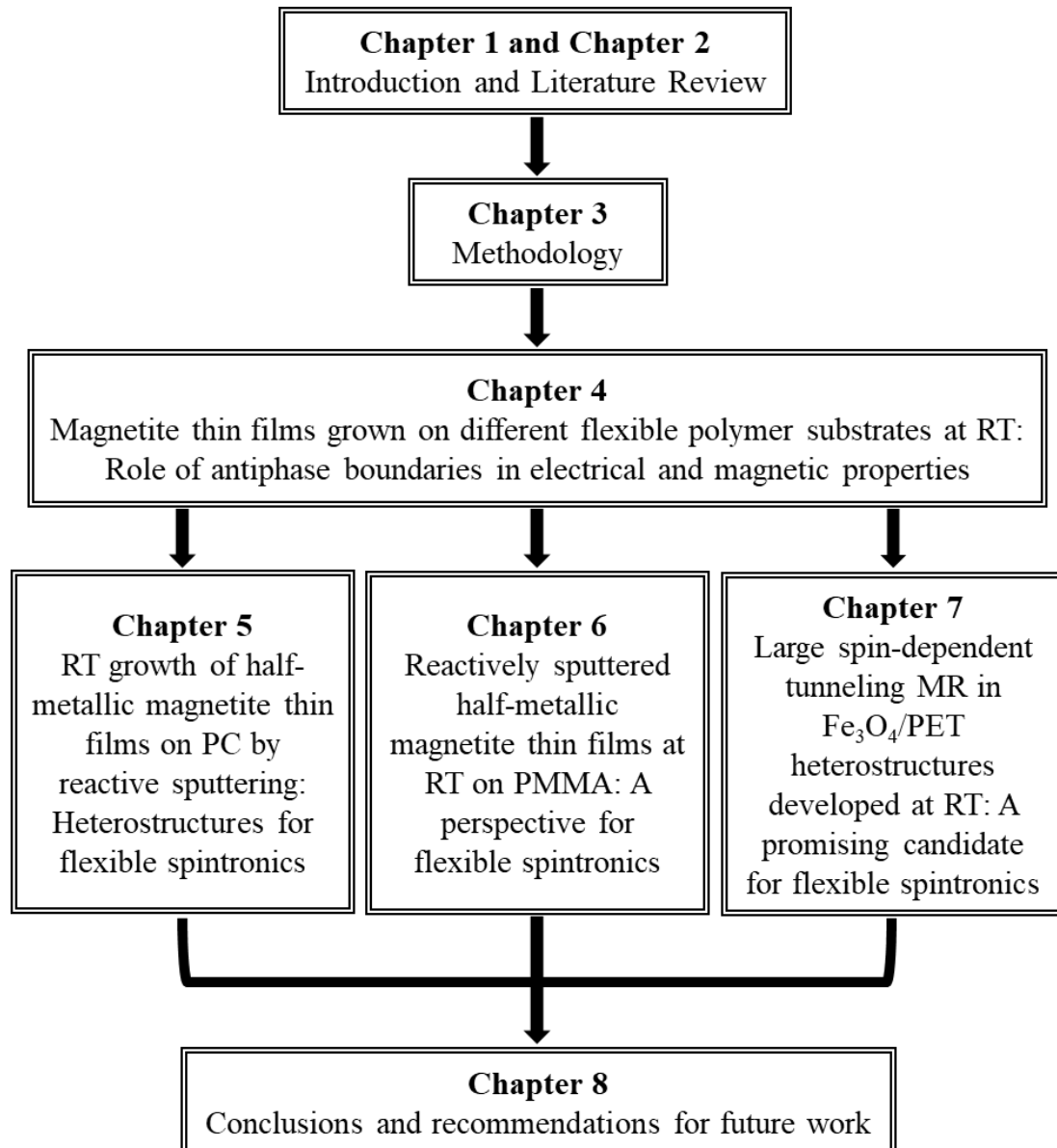


Figure 1.1 Overall thesis structure.

Chapter 1 describes the brief introduction on the spintronics and its possible applications, materials used and the importance of Fe₃O₄ into the new generation of spintronics. Then, the details of the problem statement, objectives, scopes, and the significance of the study have thoroughly stated.

Chapter 2 denotes the literature reviews of the topics of interest in this thesis. In this chapter, the detailed information of the conventional and to date technologies of the Fe₃O₄-based materials through different approaches are comprehensively discussed. The limitations of various techniques and the materials together with several

forms of Fe_3O_4 are well addressed. The intervention of the flexible spintronics technology and the techniques of producing Fe_3O_4 -based materials are also conferred. This Chapter also deliberates the advantageous and limitations of the current flexible and wearable spin-dependent electronic systems.

Chapter 3 emphases on the materials selected, technique for producing free-standing flexible polymer substrates and the development of Fe_3O_4 thin films on them. Characterization approaches and their working principles are also discussed in detail.

Chapter 4 discusses the development of Fe_3O_4 thin films with a thickness of 100 nm on as produced flexible PC, PMMA, and PET substrates through reactive RF sputtering technique at 300 K by flowing O_2 and Ar together in different ratios. The effect of various O_2 concentrations on the overall growth of iron oxides and their distinct phases are thoroughly explained. The successfully developed $\text{Fe}_3\text{O}_4/\text{PC}$, $\text{Fe}_3\text{O}_4/\text{PMMA}$, and $\text{Fe}_3\text{O}_4/\text{PET}$ heterostructures were further characterized and their structural, compositional, electrical, and magnetic properties are discussed.

Chapter 5 describes in detail the room-temperature growth of $\text{Fe}_3\text{O}_4/\text{PC}$ heterostructures with different t_d through the same technique. The morphological, chemical, electrical, and magnetic transport features of these heterostructures are discussed in terms of the Fe_3O_4 film thickness and its other structural features. Additionally, the $\text{Fe}_3\text{O}_4/\text{PC}$ heterostructure which showed superior characteristics was exploited further for its flexibility under several bending conditions are also discussed.

In **Chapter 6**, the half-metallic Fe_3O_4 thin films of different thicknesses coated on flexible PMMA substrates by reactive RF sputtering at 300 K with respect to the variable t_d , the structural, morphological, and chemical stoichiometry of these heterostructures are discussed. The electric and magnetic transport properties showing that the developed assembly of Fe_3O_4 on PMMA maintains the sole features of magnetite under bending and cyclability tests are also explained.

On the other hand, **Chapter 7** discusses the development of room-temperature stable half-metallic nanocrystalline Fe_3O_4 thin films, with the thicknesses of 50, 100, 200, and 400 nm on flexible PET substrates, by reactive RF sputtering. The explanation of the structural properties of $\text{Fe}_3\text{O}_4/\text{PET}$ heterostructures, their electrical and magnetic characteristics are conferred in this Chapter. Furthermore, the control of AFM-coupled APBs on the transport properties, due to the tunnelling of spin-polarized electrons through the films in $\text{Fe}_3\text{O}_4/\text{PET}$ heterostructures are discussed in detail. In addition, flexibility tests, to examine resistivity, M-H and MR at 300 K, with 90° and 45° bent angles and cyclability experiments to validate the reproducibility and tunability of these characteristics are also explained.

Finally, **Chapter 8** states the general conclusion for each Chapter consisted in the thesis. The suggestion and recommendation for the future work have also discussed in this Chapter.

REFERENCES

- Akay, S. K., Peksoz, A. and Kara, A. (2018) Magnetic Responses of Divinylbenzene- Fe_3O_4 Composite Film Deposited by Free Radical Polymerization Method. *Journal of Superconductivity and Novel Magnetism*, 31(3), pp. 849-854.
- Alers, G., Golding, B., Kortan, A., Haddon, R. and Theil, F. (1992) Existence of an orientational electric dipolar response in C_{60} single crystals. *Science*, 257(5069), pp. 511-514.
- Ali, U., Karim, K. J. B. A. and Buang, N. A. (2015) A review of the properties and applications of poly (methyl methacrylate)(PMMA). *Polymer Reviews*, 55(4), pp. 678-705.
- Ali, Z. I., Radwan, S. I., Shehata, M. M., Ghazy, O. A. and Saleh, H. H. (2021) Structural, optical and electrical properties of PVC/Au thin films prepared by sputtering process. *Optical and Quantum Electronics*, 53(5), pp. 241.
- Allhoff, F., Lin, P. and Moore, D. (2009) *What is nanotechnology and why does it matter?: from science to ethics*, John Wiley & Sons.
- Alonso, J., Rasines, I. and Soubeyroux, J. (1990) Tristrontium dialuminum hexaoxide: an intricate superstructure of perovskite. *Inorganic chemistry*, 29(23), pp. 4768-4771.
- Alraddadi, S., Hines, W., Yilmaz, T., Gu, G. and Sinkovic, B. (2016) Structural phase diagram for ultra-thin epitaxial $\text{Fe}_3\text{O}_4/\text{MgO}(001)$ films: thickness and oxygen pressure dependence. *Journal of Physics: Condensed Matter*, 28(11), pp. 115402.
- Alvarado, S., Eib, W., Meier, F., Pierce, D., Sattler, K., Siegmann, H. and Remeika, J. (1975) Observation of spin-polarized electron levels in ferrites. *Physical review letters*, 34(6), pp. 319.
- An, F., Qu, K., Zhong, G., Dong, Y., Ming, W., Zi, M., Liu, Z., Wang, Y., Qi, B. and Ding, Z. (2020) Highly Flexible and Twistable Freestanding Single Crystalline Magnetite Film with Robust Magnetism. *Advanced Functional Materials*, pp. 2003495.

- An, Q., Lv, F., Liu, Q., Han, C., Zhao, K., Sheng, J., Wei, Q., Yan, M. and Mai, L. (2014) Amorphous vanadium oxide matrixes supporting hierarchical porous Fe₃O₄/graphene nanowires as a high-rate lithium storage anode. *Nano letters*, *14*(11), pp. 6250-6256.
- Anguelouch, A., Gupta, A., Xiao, G., Abraham, D., Ji, Y., Ingvarsson, S. and Chien, C. (2001) Near-complete spin polarization in atomically-smooth chromium-dioxide epitaxial films prepared using a CVD liquid precursor. *Physical Review B*, *64*(18), pp. 180408.
- Anthony, J. W. (1990) *Handbook of mineralogy*, Mineral Data Publishing.
- Antonov, V., Harmon, B. and Yaresko, A. (2003) Electronic structure and x-ray magnetic circular dichroism in Fe₃O₄ and Mn-, Co-, or Ni-substituted Fe₃O₄. *Physical Review B*, *67*(2), pp. 024417.
- Aoshima, K.-i. and Wang, S. X. (2002) Epitaxial growth and characterization of Fe₃O₄ on Ru underlayer. *Journal of applied physics*, *91*(10), pp. 7146-7148.
- Aoshima, K.-i. and Wang, S. X. (2003) Fe₃O₄ and its magnetic tunneling junctions grown by ion beam deposition. *Journal of applied physics*, *93*(10), pp. 7954-7956.
- Aragón, R., Gehring, P. and Shapiro, S. (1993) Stoichiometry, percolation, and Verwey ordering in magnetite. *Physical review letters*, *70*(11), pp. 1635.
- Arora, S., Sofin, R., Nolan, A. and Shvets, I. (2005a) Antiphase boundaries induced exchange coupling in epitaxial Fe₃O₄ thin films. *Journal of Magnetism and Magnetic Materials*, *286*, pp. 463-467.
- Arora, S., Sofin, R. and Shvets, I. (2005b) Magnetoresistance enhancement in epitaxial magnetite films grown on vicinal substrates. *Physical Review B*, *72*(13), pp. 134404.
- Ashfold, M. N., Claeysens, F., Fuge, G. M. and Henley, S. J. (2004) Pulsed laser ablation and deposition of thin films. *Chemical Society Reviews*, *33*(1), pp. 23-31.
- Auffan, M., Rose, J., Bottero, J.-Y., Lowry, G. V., Jolivet, J.-P. and Wiesner, M. R. (2009) Towards a definition of inorganic nanoparticles from an environmental, health and safety perspective. *Nature nanotechnology*, *4*(10), pp. 634.
- Bader, S. and Parkin, S. (2010) Spintronics. *Annu. Rev. Condens. Matter Phys.*, *1*(1), pp. 71-88.

- Baibich, M. N., Broto, J. M., Fert, A., Van Dau, F. N., Petroff, F., Etienne, P., Creuzet, G., Friederich, A. and Chazelas, J. (1988) Giant magnetoresistance of (001) Fe/(001) Cr magnetic superlattices. *Physical review letters*, 61(21), pp. 2472.
- Bakun, A., Zakharchenya, B., Rogachev, A., Tkachuk, M. and Fleisher, V. (1984) Observation of a surface photocurrent caused by optical orientation of electrons in a semiconductor. *JETP Lett*, 40(11).
- Balashev, V., Korobtsov, V., Pisarenko, T. and Chebotkevich, L. (2011) Growth of Fe₃O₄ films on the Si(111) surface covered by a thin SiO₂ layer. *Technical Physics*, 56(10), pp. 1501.
- Barbara, L. D. Louisiana State University, Christine M. Clark, Eastern Michigan University. *X-ray Powder Diffraction (XRD) Geochemical Instrumentation and Analysis*.
- Barnaś, J., Fuss, A., Camley, R., Grünberg, P. and Zinn, W. (1990) Novel magnetoresistance effect in layered magnetic structures: Theory and experiment. *Physical Review B*, 42(13), pp. 8110.
- Barraud, C., Deranlot, C., Seneor, P., Mattana, R., Dlubak, B., Fusil, S., Bouzeshouane, K., Deneuve, D., Petroff, F. and Fert, A. (2010) Magnetoresistance in magnetic tunnel junctions grown on flexible organic substrates. *Applied Physics Letters*, 96(7), pp. 072502.
- Bäumer, M., Libuda, J. and Freund, H.-J. (1995) The temperature dependent growth mode of nickel on the basal plane of graphite. *Surface science*, 327(3), pp. 321-329.
- Bedoya-Pinto, A., Donolato, M., Gobbi, M., Hueso, L. E. and Vavassori, P. (2014) Flexible spintronic devices on Kapton. *Applied Physics Letters*, 104(6), pp. 062412.
- Berger, L. (1996) Emission of spin waves by a magnetic multilayer traversed by a current. *Physical Review B*, 54(13), pp. 9353.
- Berkowitz, A., Mitchell, J., Carey, M., Young, A., Zhang, S., Spada, F., Parker, F., Hutten, A. and Thomas, G. (1992) Giant magnetoresistance in heterogeneous Cu-Co alloys. *Physical review letters*, 68(25), pp. 3745.
- Bhat, S. G. and Kumar, P. A. (2014) Room temperature electrical spin injection into GaAs by an oxide spin injector. *Scientific reports*, 4, pp. 5588.

- Bhat, S. G. and Kumar, P. A. (2016) Enhanced spin accumulation in Fe₃O₄ based spin injection devices below the Verwey transition. *Materials Research Express*, 3(12), pp. 125905.
- Bhattacharya, P., Fornari, R. and Kamimura, H. (2011) *Comprehensive Semiconductor Science and Technology: Online Version*, Newnes.
- Bibes, M. and Barthelemy, A. (2007) Oxide spintronics. *IEEE transactions on electron devices*, 54(5), pp. 1003-1023.
- Binasch, G., Grünberg, P., Saurenbach, F. and Zinn, W. (1989) Enhanced magnetoresistance in layered magnetic structures with antiferromagnetic interlayer exchange. *Physical Review B*, 39(7), pp. 4828.
- Bitla, Y. and Chu, Y.-H. (2017) MICATronics: A new platform for flexible X-tronics. *FlatChem*, 3, pp. 26-42.
- Bobo, J., Basso, D., Snoeck, E., Gatel, C., Hrabovsky, D., Gauffier, J., Ressler, L., Mamy, R., Visnovsky, S. and Hamrle, J. (2001) Magnetic behavior and role of the antiphase boundaries in Fe₃O₄ epitaxial films sputtered on MgO (001). *The European Physical Journal B-Condensed Matter and Complex Systems*, 24(1), pp. 43-49.
- Bohra, M., Prasad, K. E., Bollina, R., Sahoo, S. and Kumar, N. (2016) Characterizing the phase purity of nanocrystalline Fe₃O₄ thin films using Verwey transition. *Journal of Magnetism and Magnetic Materials*, 418, pp. 137-142.
- Bohra, M., Prasad, S., Venketaramani, N., Kumar, N., Sahoo, S. and Krishnan, R. (2009) Magnetic properties of magnetite thin films close to the Verwey transition. *Journal of Magnetism and Magnetic Materials*, 321(22), pp. 3738-3741.
- Bohra, M., Roy Chowdhury, D., Bobo, J.-F. and Singh, V. (2019) Anomalous electric transport across Verwey transition in nanocrystalline Fe₃O₄ thin films. *Journal of applied physics*, 125(1), pp. 013901.
- Bohra, M. and Sahoo, S. (2017) Large magnetocaloric effect at Verwey point in nanocrystalline Fe₃O₄ thin films. *Journal of Alloys and Compounds*, 699, pp. 1118-1121.
- Bollero, A., Ziese, M., Höhne, R., Semmelhack, H., Köhler, U., Setzer, A. and Esquinazi, P. (2005) Influence of thickness on microstructural and magnetic properties in Fe₃O₄ thin films produced by PLD. *Journal of Magnetism and Magnetic Materials*, 285(1-2), pp. 279-289.

- Boothman, C., Sánchez, A. M. and Van Dijken, S. (2007) Structural, magnetic, and transport properties of $\text{Fe}_3\text{O}_4/\text{Si}$ (111) and $\text{Fe}_3\text{O}_4/\text{Si}$ (001). *Journal of applied physics*, 101(12), pp. 123903.
- Bowen, M., Bibes, M., Barthélémy, A., Contour, J.-P., Anane, A., Lemaitre, Y. and Fert, A. (2003) Nearly total spin polarization in $\text{La}_{2/3}\text{Sr}_{1/3}\text{MnO}_3$ from tunneling experiments. *Applied Physics Letters*, 82(2), pp. 233-235.
- Brabers, V., Walz, F. and Kronmüller, H. (1998) Impurity effects upon the Verwey transition in magnetite. *Physical Review B*, 58(21), pp. 14163.
- Bruce, I. J. and Sen, T. (2005) Surface modification of magnetic nanoparticles with alkoxysilanes and their application in magnetic bioseparations. *Langmuir*, 21(15), pp. 7029-7035.
- Bruski, P., Manzke, Y., Farshchi, R., Brandt, O., Herfort, J. and Ramsteiner, M. (2013) All-electrical spin injection and detection in the $\text{Co}_2\text{FeSi}/\text{GaAs}$ hybrid system in the local and non-local configuration. *Applied Physics Letters*, 103(5), pp. 052406.
- Burghoorn, M., Roosen-Melsen, D., de Riet, J., Sabik, S., Vroon, Z., Yakimets, I. and Buskens, P. (2013) Single layer broadband anti-reflective coatings for plastic substrates produced by full wafer and roll-to-roll step-and-flash nano-imprint lithography. *Materials*, 6(9), pp. 3710-3726.
- Bychkov, Y. A. and Rashba, É. I. (1984) Properties of a 2D electron gas with lifted spectral degeneracy. *JETP Lett*, 39(2), pp. 78.
- Cadore, Í. R., Ambrosi, A., Cardozo, N. S. M. and Tessaro, I. C. (2019) Phase separation behavior of poly(ethylene terephthalate)/(trifluoroacetic acid/dichloromethane)/water system for wet phase inversion membrane preparation. *Journal of applied polymer science*, 136(13), pp. 47263.
- Cao, S.-W., Zhu, Y.-J., Ma, M.-Y., Li, L. and Zhang, L. (2008) Hierarchically nanostructured magnetic hollow spheres of Fe_3O_4 and $\gamma\text{-Fe}_2\text{O}_3$: preparation and potential application in drug delivery. *The Journal of Physical Chemistry C*, 112(6), pp. 1851-1856.
- Caruso, F. (2001) Nanoengineering of particle surfaces. *Advanced Materials*, 13(1), pp. 11-22.
- Chambers, S. A. (2000) Epitaxial growth and properties of thin film oxides. *Surface science reports*, 39(5-6), pp. 105-180.

- Chambers, S. A., Thevuthasan, S. and Joyce, S. A. (2000) Surface structure of MBE-grown Fe₃O₄ (001) by X-ray photoelectron diffraction and scanning tunneling microscopy. *Surface science*, 450(1-2), pp. L273-L279.
- Chang, C., Regan, B., Mickelson, W., Ritchie, R. and Zettl, A. (2003) Probing structural phase transitions of crystalline C60 via resistivity measurements of metal film overlayers. *Solid state communications*, 128(9-10), pp. 359-363.
- Chapline, M. G. and Wang, S. X. (2005) Observation of the Verwey transition in thin magnetite films. *Journal of applied physics*, 97(12), pp. 123901.
- Chen, C., Idzerda, Y., Lin, H.-J., Smith, N., Meigs, G., Chaban, E., Ho, G., Pellegrin, E. and Sette, F. (1995) Experimental confirmation of the X-ray magnetic circular dichroism sum rules for iron and cobalt. *Physical review letters*, 75(1), pp. 152.
- Chen, J.-R., Odenthal, P. M., Swartz, A. G., Floyd, G. C., Wen, H., Luo, K. Y. and Kawakami, R. K. (2013) Control of Schottky barriers in single layer MoS₂ transistors with ferromagnetic contacts. *Nano letters*, 13(7), pp. 3106-3110.
- Chen, Y., Sun, J., Han, Y., Xie, X., Shen, J., Rong, C., He, S. and Shen, B. (2008) Microstructure and magnetic properties of strained Fe₃O₄ films. *Journal of applied physics*, 103(7), pp. 07D703.
- Chen, Y. f., Mei, Y., Kaltofen, R., Mönch, J. I., Schumann, J., Freudenberger, J., Klauß, H. J. and Schmidt, O. G. (2008) Towards Flexible Magnetoelectronics: Buffer-Enhanced and Mechanically Tunable GMR of Co/Cu Multilayers on Plastic Substrates. *Advanced Materials*, 20(17), pp. 3224-3228.
- Cheung, W., Chiu, P. L., Parajuli, R. R., Ma, Y., Ali, S. R. and He, H. (2009) Fabrication of high performance conducting polymer nanocomposites for biosensors and flexible electronics: summary of the multiple roles of DNA dispersed and functionalized single walled carbon nanotubes. *Journal of Materials Chemistry*, 19(36), pp. 6465-6480.
- Chien, C., Xiao, J. Q. and Jiang, J. S. (1993) Giant negative magnetoresistance in granular ferromagnetic systems. *Journal of applied physics*, 73(10), pp. 5309-5314.
- Choi, C. H., Lee, D. J., Sung, J.-H., Lee, M. W., Lee, S.-G., Park, S.-G., Lee, E.-H. and Beom-Hoan, O. (2010) A study of AFM-based scratch process on polycarbonate surface and grating application. *Applied Surface Science*, 256(24), pp. 7668-7671.

- Chung, K. W., Kim, K. B., Han, S.-H. and Lee, H. (2005) Novel synthesis and electrochemical characterization of nano-sized cellular Fe₃O₄ thin film. *Electrochemical and Solid State Letters*, 8(5), pp. A259.
- Claydon, J., Xu, Y., Tselepi, M., Bland, J. and Van der Laan, G. (2004) Direct Observation of a Bulklike Spin Moment at the Fe / GaAs(100) – 4 × 6 Interface. *Physical review letters*, 93(3), pp. 037206.
- Coey, J., Berkowitz, A., Balcells, L., Putris, F. and Barry, A. (1998a) Magnetoresistance of chromium dioxide powder compacts. *Physical review letters*, 80(17), pp. 3815.
- Coey, J., Berkowitz, A., Balcells, L., Putris, F. and Parker, F. (1998b) Magnetoresistance of magnetite. *Applied Physics Letters*, 72(6), pp. 734-736.
- Coey, J. and Sanvito, S. (2004) Magnetic semiconductors and half-metals. *Journal of Physics D: Applied Physics*, 37(7), pp. 988.
- Coey, J. and Venkatesan, M. (2002) Half-metallic ferromagnetism: Example of CrO₂. *Journal of applied physics*, 91(10), pp. 8345-8350.
- Cornell, R. M. and Schwertmann, U. (2003) *The iron oxides: structure, properties, reactions, occurrences and uses*, John Wiley & Sons.
- Cushing, B. L., Kolesnichenko, V. L. and O'Connor, C. J. (2004) Recent advances in the liquid-phase syntheses of inorganic nanoparticles. *Chemical reviews*, 104(9), pp. 3893-3946.
- D'yakonov, M. and Perel, V. (1971) Possibility of orienting electron spins with current. *Soviet Journal of Experimental and Theoretical Physics Letters*, 13, pp. 467.
- Dai, J. and Tang, J. (2001) Junction-like magnetoresistance of intergranular tunneling in field-aligned chromium dioxide powders. *Physical Review B*, 63(5), pp. 054434.
- Dai, J., Tang, J., Xu, H., Spinu, L., Wang, W., Wang, K., Kumbhar, A., Li, M. and Diebold, U. (2000) Characterization of the natural barriers of intergranular tunnel junctions: Cr₂O₃ surface layers on CrO₂ nanoparticles. *Applied Physics Letters*, 77(18), pp. 2840-2842.
- Dankert, A., Langouche, L., Kamalakar, M. V. and Dash, S. P. (2014) High-performance molybdenum disulfide field-effect transistors with spin tunnel contacts. *ACS nano*, 8(1), pp. 476-482.

- Datta, R., Loukya, B., Li, N. and Gupta, A. (2012) Structural features of epitaxial NiFe₂O₄ thin films grown on different substrates by direct liquid injection chemical vapor deposition. *Journal of crystal growth*, 345(1), pp. 44-50.
- Datta, S. and Das, B. (1990) Electronic analog of the electro-optic modulator. *Applied Physics Letters*, 56(7), pp. 665-667.
- De Groot, R., Mueller, F., Van Engen, P. and Buschow, K. (1983) New class of materials: half-metallic ferromagnets. *Physical review letters*, 50(25), pp. 2024.
- De Teresa, J. M., Barthelemy, A., Fert, A., Contour, J. P., Montaigne, F. and Seneor, P. (1999) Role of metal-oxide interface in determining the spin polarization of magnetic tunnel junctions. *Science*, 286(5439), pp. 507-509.
- Dediu, V., Murgia, M., Maticotta, F., Taliani, C. and Barbanera, S. (2002) Room temperature spin polarized injection in organic semiconductor. *Solid state communications*, 122(3-4), pp. 181-184.
- Dedkov, Y. S., Fonin, M., Rüdiger, U. and Laubschat, C. (2008) Graphene-protected iron layer on Ni (111). *Applied Physics Letters*, 93(2), pp. 022509.
- Dedkov, Y. S., Generalov, A., Voloshina, E. and Fonin, M. (2011) Structural and electronic properties of Fe₃O₄/graphene/Ni(111) junctions. *physica status solidi (RRL)–Rapid Research Letters*, 5(7), pp. 226-228.
- Dedkov, Y. S., Rüdiger, U. and Güntherodt, G. (2002) Evidence for the half-metallic ferromagnetic state of Fe₃O₄ by spin-resolved photoelectron spectroscopy. *Physical Review B*, 65(6), pp. 064417.
- Deng, B., Hsu, P.-C., Chen, G., Chandrashekar, B., Liao, L., Ayitimuda, Z., Wu, J., Guo, Y., Lin, L. and Zhou, Y. (2015) Roll-to-roll encapsulation of metal nanowires between graphene and plastic substrate for high-performance flexible transparent electrodes. *Nano letters*, 15(6), pp. 4206-4213.
- Dho, J., Kim, B. and Ki, S. (2016) Substrate Effects on In-Plane Magnetic Anisotropy and Verwey Transition Temperatures of (100) Magnetite (Fe₃O₄) Films. *IEEE Transactions on Magnetics*, 52(7), pp. 1-4.
- Dileep, K., Loukya, B., Pachauri, N., Gupta, A. and Datta, R. (2014) Probing optical band gaps at the nanoscale in NiFe₂O₄ and CoFe₂O₄ epitaxial films by high resolution electron energy loss spectroscopy. *Journal of applied physics*, 116(10), pp. 103505.

- Ding, J., Zhang, D., Arita, M., Ikoma, Y., Nakamura, K., Saito, K. and Guo, Q. (2011) Growth and characterization of Fe₃O₄ films. *Materials Research Bulletin*, 46(12), pp. 2212-2216.
- Djayaprawira, D. D., Tsunekawa, K., Nagai, M., Maehara, H., Yamagata, S., Watanabe, N., Yuasa, S., Suzuki, Y. and Ando, K. (2005) 230% room-temperature magnetoresistance in CoFeB/MgO/CoFeB magnetic tunnel junctions. *Applied Physics Letters*, 86(9), pp. 092502.
- Dolui, K., Narayan, A., Rungger, I. and Sanvito, S. (2014) Efficient spin injection and giant magnetoresistance in Fe/MoS₂/Fe junctions. *Physical Review B*, 90(4), pp. 041401.
- Douglas, F. J., MacLaren, D. A. and Murrie, M. (2012) A study of the role of the solvent during magnetite nanoparticle synthesis: tuning size, shape and self-assembly. *Rsc Advances*, 2(21), pp. 8027-8035.
- Duan, H., Chen, X., Li, B. and Liang, J. (2010) Growth morphology study of cathodically electrodeposited Fe₃O₄ thin films at elevated temperatures. *Materials Research Bulletin*, 45(11), pp. 1696-1702.
- Dulli, H., Plummer, E. W., Dowben, P. A., Choi, J. and Liou, S.-H. (2000) Surface electronic phase transition in colossal magnetoresistive manganese perovskites: La_{0.65}Sr_{0.35}MnO₃. *Applied Physics Letters*, 77(4), pp. 570-572.
- Ebina, Y., Akiho, T., Liu, H.-x., Yamamoto, M. and Uemura, T. (2014) Effect of CoFe insertion in Co₂MnSi/CoFe/n-GaAs junctions on spin injection properties. *Applied Physics Letters*, 104(17), pp. 172405.
- Eerenstein, W., Kalev, L., Niesen, L., Palstra, T. and Hibma, T. (2003a) Magnetoresistance and superparamagnetism in magnetite films on MgO and MgAl₂O₄. *Journal of Magnetism and Magnetic Materials*, 258, pp. 73-76.
- Eerenstein, W., Palstra, T., Hibma, T. and Celotto, S. (2002a) Origin of the increased resistivity in epitaxial Fe₃O₄ films. *Physical Review B*, 66(20), pp. 201101.
- Eerenstein, W., Palstra, T., Hibma, T. and Celotto, S. (2003b) Diffusive motion of antiphase domain boundaries in Fe₃O₄ films. *Physical Review B*, 68(1), pp. 014428.
- Eerenstein, W., Palstra, T., Saxena, S. and Hibma, T. (2002b) Spin-polarized transport across sharp antiferromagnetic boundaries. *Physical review letters*, 88(24), pp. 247204.

- Fabian, J., Matos-Abiague, A., Ertler, C., Stano, P. and Zutic, I. (2007) Semiconductor spintronics. *arXiv preprint arXiv:0711.1461*.
- Fan, T., Pan, D. and Zhang, H. (2011) Study on formation mechanism by monitoring the morphology and structure evolution of nearly monodispersed Fe₃O₄ submicroparticles with controlled particle sizes. *Industrial & Engineering Chemistry Research*, 50(15), pp. 9009-9018.
- Farzad, N. and Alain, N. (2010) *Nanomagnetism and spintronics: fabrication, materials, characterization and applications*, World Scientific.
- Feng, C., Liu, K., Wu, J. S., Liu, L., Cheng, J. S., Zhang, Y., Sun, Y., Li, Q., Fan, S. and Jiang, K. (2010) Flexible, stretchable, transparent conducting films made from superaligned carbon nanotubes. *Advanced Functional Materials*, 20(6), pp. 885-891.
- Ferguson, J., Arikan, G., Dale, D., Woll, A. and Brock, J. (2009) Measurements of surface diffusivity and coarsening during pulsed laser deposition. *Physical Review Letters*, 103(25), pp. 256103.
- Ferhat, M. and Yoh, K. (2007) High quality Fe_{3-δ}O₄/InAs hybrid structure for electrical spin injection. *Applied Physics Letters*, 90(11), pp. 112501.
- Fleet, M. (1981) *Acta Crystallogr. B. Sect. B Struct. Crystallogr. Cryst. Chem.*, 37, pp. 917.
- Foerster, M., Gutierrez, D., Rebled, J., Arbelo, E., Rigato, F., Jourdan, M., Peiró, F. and Fontcuberta, J. (2012) Electric transport through nanometric CoFe₂O₄ thin films investigated by conducting atomic force microscopy. *Journal of applied physics*, 111(1), pp. 013904.
- Fonin, M., Dedkov, Y. S., Mayer, J., Rüdiger, U. and Güntherodt, G. (2003) Preparation, structure, and electronic properties of Fe₃O₄ films on the Fe(110)/Mo(110)/Al₂O₃(112⁻0) substrate. *Physical Review B*, 68(4), pp. 045414.
- Friák, M., Schindlmayr, A. and Scheffler, M. (2007) Ab initio study of the half-metal to metal transition in strained magnetite. *New journal of physics*, 9(1), pp. 5.
- Fritsch, D. and Ederer, C. (2011) Effect of epitaxial strain on the cation distribution in spinel ferrites CoFe₂O₄ and NiFe₂O₄: A density functional theory study. *Applied Physics Letters*, 99(8), pp. 081916.

- Fujii, T., De Groot, F., Sawatzky, G., Voogt, F., Hibma, T. and Okada, K. (1999) In situ XPS analysis of various iron oxide films grown by NO₂-assisted molecular-beam epitaxy. *Physical Review B*, 59(4), pp. 3195.
- Fujimori, A., Saeki, M., Kimizuka, N., Taniguchi, M. and Suga, S. (1986) Photoemission satellites and electronic structure of Fe₂O₃. *Physical Review B*, 34(10), pp. 7318.
- Furubayashi, T. (2003) Magnetoresistance of magnetite films prepared by reactive evaporation. *Journal of Applied Physics*, 93(10), pp. 8026-8028.
- Gao, Y. and Chambers, S. (1997) Heteroepitaxial growth of α -Fe₂O₃, γ -Fe₂O₃ and Fe₃O₄ thin films by oxygen-plasma-assisted molecular beam epitaxy. *Journal of crystal growth*, 174(1-4), pp. 446-454.
- Gao, Y. and Chambers, S. A. (1997) Heteroepitaxial growth of α -Fe₂O₃, γ -Fe₂O₃ and Fe₃O₄ thin films by oxygen-plasma-assisted molecular beam epitaxy. *Journal of crystal growth*, 174(1-4), pp. 446-454.
- Gao, Y., Kim, Y., Chambers, S. and Bai, G. (1997) Synthesis of epitaxial films of Fe₃O₄ and α -Fe₂O₃ with various low-index orientations by oxygen-plasma-assisted molecular beam epitaxy. *Journal of Vacuum Science & Technology A: Vacuum, Surfaces, and Films*, 15(2), pp. 332-339.
- Gass, J., Poddar, P., Almand, J., Srinath, S. and Srikanth, H. (2006) Superparamagnetic polymer nanocomposites with uniform Fe₃O₄ nanoparticle dispersions. *Advanced Functional Materials*, 16(1), pp. 71-75.
- Geprägs, S., Mannix, D., Opel, M., Goennenwein, S. T. and Gross, R. (2013) Converse magnetoelectric effects in Fe₃O₄/BaTiO₃ multiferroic hybrids. *Physical Review B*, 88(5), pp. 054412.
- Gilks, D., Kepaptsoglou, D., McKenna, K., Lari, L., Ramasse, Q., Matsuzaki, K., Susaki, T. and Lazarov, V. (2015) Atomic study of Fe₃O₄/SrTiO₃ Interface. *Microscopy and Microanalysis*, 21(S3), pp. 1299-1300.
- Gilks, D., McKenna, K. P., Nedelkoski, Z., Kuerbanjiang, B., Matsuzaki, K., Susaki, T., Lari, L., Kepaptsoglou, D., Ramasse, Q. and Tear, S. (2016) Polar Spinel-Perovskite Interfaces: an atomistic study of Fe₃O₄ (111)/SrTiO₃ (111) structure and functionality. *Scientific reports*, 6, pp. 29724.
- Goktas, A., Mutlu, I. and Yamada, Y. (2013) Influence of Fe-doping on the structural, optical, and magnetic properties of ZnO thin films prepared by sol-gel method. *Superlattices and Microstructures*, 57, pp. 139-149.

- Gomes, G., Bueno, T., Parreiras, D., Abreu, G., de Siervo, A., Cezar, J., Pfannes, H.-D. and Paniago, R. (2014) Magnetic moment of Fe₃O₄ films with thicknesses near the unit-cell size. *Physical Review B*, 90(13), pp. 134422.
- Gong, G., Gupta, A., Xiao, G., Qian, W. and Dravid, V. (1997) Magnetoresistance and magnetic properties of epitaxial magnetite thin films. *Physical Review B*, 56(9), pp. 5096.
- Gooth, J., Zierold, R., Gluschke, J. G., Boehnert, T., Edinger, S., Barth, S. and Nielsch, K. (2013) Gate voltage induced phase transition in magnetite nanowires. *Applied Physics Letters*, 102(7), pp. 073112.
- Goyal, R. N., Kaur, D. and Pandey, A. K. (2010) Substrate dependent structural and magnetic properties of pulsed laser deposited Fe₃O₄ thin films. *Journal of nanoscience and nanotechnology*, 10(12), pp. 8018-8025.
- Gridin, V., Hearne, G. and Honig, J. (1996) Magnetoresistance extremum at the first-order Verwey transition in magnetite (Fe₃O₄). *Physical Review B*, 53(23), pp. 15518.
- Grünberg, P., Schreiber, R., Pang, Y., Brodsky, M. and Sowers, H. (1986) Layered magnetic structures: Evidence for antiferromagnetic coupling of Fe layers across Cr interlayers. *Physical review letters*, 57(19), pp. 2442.
- Gunnarsson, O. and Schönhammer, K. (1983) Electron spectroscopies for Ce compounds in the impurity model. *Physical Review B*, 28(8), pp. 4315.
- Gupta, A., Li, X. and Xiao, G. (2000) Magnetic and transport properties of epitaxial and polycrystalline chromium dioxide thin films. *Journal of applied physics*, 87(9), pp. 6073-6078.
- Gupta, R., Ghosh, K. and Kahol, P. (2010) Room temperature ferromagnetic multilayer thin film based on indium oxide and iron oxide for transparent spintronic applications. *Materials Letters*, 64(18), pp. 2022-2024.
- Gutiérrez, D., Foerster, M., Fina, I., Fontcuberta, J., Fritsch, D. and Ederer, C. (2012) Dielectric response of epitaxially strained CoFe₂O₄ spinel thin films. *Physical Review B*, 86(12), pp. 125309.
- Hall, K. C. and Flatte, M. E. (2006) Performance of a spin-based insulated gate field effect transistor. *Applied Physics Letters*, 88(16), pp. 162503.

- Hamie, A., Dumont, Y., Popova, E., Fouchet, A., Warot-Fonrose, B., Gatel, C., Chikoidze, E., Scola, J., Berini, B. and Keller, N. (2012) Investigation of high quality magnetite thin films grown on SrTiO₃ (001) substrates by pulsed laser deposition. *Thin Solid Films*, 525, pp. 115-120.
- Hari Babu, V., Govind, R., Schindler, K.-M., Welke, M. and Denecke, R. (2013) Epitaxial growth and magnetic properties of ultrathin iron oxide films on BaTiO₃ (001). *Journal of applied physics*, 114(11), pp. 113901.
- Hassan, S. S., Xu, Y., Ahmad, E. and Lu, Y. (2007) Transport and magneto-transport characteristics of Fe₃O₄/GaAs hybrid structure. *IEEE transactions on magnetics*, 43(6), pp. 2875-2877.
- Hassan, S. S., Xu, Y., Wu, J. and Thompson, S. M. (2009) Epitaxial Growth and Magnetic Properties of Half-Metallic Fe₃O₄ on Si (100) Using MgO Buffer Layer. *IEEE Transactions on Magnetism*, 45(10), pp. 4357-4359.
- He, C., Wu, S., Zhao, N., Shi, C., Liu, E. and Li, J. (2013) Carbon-encapsulated Fe₃O₄ nanoparticles as a high-rate lithium ion battery anode material. *ACS nano*, 7(5), pp. 4459-4469.
- He, Z., Koza, J. A., Mu, G., Miller, A. S., Bohannon, E. W. and Switzer, J. A. (2013) Electrodeposition of Co_xFe_{3-x}O₄ Epitaxial Films and Superlattices. *Chemistry of Materials*, 25(2), pp. 223-232.
- Heusler, F. and Take, E. (1912) The nature of the Heusler alloys. *Transactions of the Faraday Society*, 8(October), pp. 169-184.
- Hibma, T., Voogt, F., Niesen, L., Van der Heijden, P., De Jonge, W., Donkers, J. and Van der Zaag, P. (1999) Anti-phase domains and magnetism in epitaxial magnetite layers. *Journal of applied physics*, 85(8), pp. 5291-5293.
- Hirohata, A., Kikuchi, M., Tezuka, N., Inomata, K., Claydon, J., Xu, Y. and Van der Laan, G. (2006) Heusler alloy/semiconductor hybrid structures. *Current Opinion in Solid State and Materials Science*, 10(2), pp. 93-107.
- Hong, J. P., Lee, S. B., Jung, Y. W., Lee, J. H., Yoon, K. S., Kim, K. W., Kim, C. O., Lee, C. H. and Jung, M. H. (2003) Room temperature formation of half-metallic Fe₃O₄ thin films for the application of spintronic devices. *Applied Physics Letters*, 83(8), pp. 1590-1592.
- Hsu, J.-H., Chen, S.-Y. and Chang, C.-R. (2002) Anomalous positive magnetoresistance in Fe₃O₄-Ag composite films. *Journal of Magnetism and Magnetic Materials*, 242, pp. 479-481.

- Hsu, J.-H., Chen, S.-Y., Chang, W.-M., Jian, T., Chang, C.-R. and Lee, S.-F. (2003) Magnetoresistance effect in Ag-Fe₃O₄ and Al-Fe₃O₄ composite films. *Journal of applied physics*, 93(10), pp. 7702-7704.
- Hu, G. and Suzuki, Y. (2002) Negative Spin Polarization of Fe₃O₄ in Magnetite/Manganite-Based Junctions. *Physical review letters*, 89(27), pp. 276601.
- Hu, X., Xu, M., Cui, X. and Zhang, S. (2007) Room-temperature magnetoresistance effects of Ag-added Fe₃O₄ films with single-domain grains. *Solid state communications*, 142(10), pp. 595-599.
- Huang, D., Chang, C., Jeng, H.-T., Guo, G., Lin, H.-J., Wu, W., Ku, H., Fujimori, A., Takahashi, Y. and Chen, C. (2004) Spin and Orbital Magnetic Moments of Fe₃O₄. *Physical review letters*, 93(7), pp. 077204.
- Huang, J., Lin, Y., Ji, M., Cong, G., Liu, H., Yu, J., Yang, B., Li, C., Zhu, C. and Xu, J. (2020) Nitrogen-doped porous carbon derived from foam polystyrene as an anode material for lithium-ion batteries. *Applied Surface Science*, 504, pp. 144398.
- Huang, P.-H., Lai, C.-H. and Huang, R. (2005) Room-temperature growth of epitaxial (111) Fe₃O₄ films with conductive Cu underlayer. *Journal of applied physics*, 97(10), pp. 10C311.
- Huang, X. and Ding, J. (2013) The structure, magnetic and transport properties of Fe₃O₄ thin films on different substrates by pulsed laser deposition. *Journal of the Korean Physical Society*, 62(12), pp. 2228-2232.
- Huang, Z., Hu, X., Xu, Y., Zhai, Y., Xu, Y., Wu, J. and Zhai, H. (2012) Magnetic properties of ultrathin single crystal Fe₃O₄ film on InAs (100) by ferromagnetic resonance. *Journal of applied physics*, 111(7), pp. 07C108.
- Huang, Z., Zhai, Y., Lu, Y., Li, G., Wong, P., Xu, Y., Xu, Y. and Zhai, H. (2008) The interface effect of the magnetic anisotropy in ultrathin epitaxial Fe₃O₄ film. *Applied Physics Letters*, 92(11), pp. 113105.
- Huang, Z., Zhai, Y., Xu, Y., Wu, J., Thompson, S. M. and Holmes, S. (2011) Growth and magnetic properties of ultrathin single crystal Fe₃O₄ film on InAs (100). *physica status solidi (a)*, 208(10), pp. 2377-2379.
- Huang, Z. C., Hu, X. F., Xu, Y. X., Zhai, Y., Xu, Y. B., Wu, J. and Zhai, H. R. (2012) Magnetic properties of ultrathin single crystal Fe₃O₄ film on InAs(100) by ferromagnetic resonance. *Journal of applied physics*, 111(7), pp. 07C108.

- Hwang, H. and Cheong, S.-W. (1997) Enhanced intergrain tunneling magnetoresistance in half-metallic CrO₂ films. *Science*, 278(5343), pp. 1607-1609.
- Im, H.-G., An, B. W., Jin, J., Jang, J., Park, Y.-G., Park, J.-U. and Bae, B.-S. (2016) A high-performance, flexible and robust metal nanotrough-embedded transparent conducting film for wearable touch screen panels. *Nanoscale*, 8(7), pp. 3916-3922.
- Iqbal, M. Z., Iqbal, M. W., Siddique, S., Khan, M. F. and Ramay, S. M. (2016) Room temperature spin valve effect in NiFe/WS₂/Co junctions. *Scientific reports*, 6(1), pp. 1-6.
- Ishibashi, S., Namikawa, T. and Satou, M. (1979) Epitaxial growth of ferromagnetic CrO₂ films in air. *Materials Research Bulletin*, 14(1), pp. 51-57.
- Ishikawa, M., Tanaka, H. and Kawai, T. (2005) Preparation of highly conductive Mn-doped Fe₃O₄ thin films with spin polarization at room temperature using a pulsed-laser deposition technique. *Applied Physics Letters*, 86(22), pp. 222504.
- Jaffari, G. H., Rumaiz, A., Woicik, J. and Shah, S. I. (2012) Influence of oxygen vacancies on the electronic structure and magnetic properties of NiFe₂O₄ thin films. *Journal of applied physics*, 111(9), pp. 093906.
- Jain, S., Adeyeye, A. and Boothroyd, C. (2005) Electronic properties of half metallic Fe₃O₄ films. *Journal of applied physics*, 97(9), pp. 093713.
- Jain, S., Adeyeye, A. and Dai, D. (2004) Magnetic properties of half-metallic Fe₃O₄ films. *Journal of applied physics*, 95(11), pp. 7237-7239.
- Jeng, H.-T., Guo, G. and Huang, D. (2004) Charge-orbital ordering and Verwey transition in magnetite. *Physical review letters*, 93(15), pp. 156403.
- Jeon, S.-H., Song, G.-D. and Hur, D.-H. (2015) Electrodeposition of magnetite on carbon steel in Fe (III)-triethanolamine solution and its corrosion behavior. *Materials transactions*, 56(7), pp. 1107-1111.
- Jeong, J. Y., Cho, Y. T. and Jung, Y. G. (2015) Refractive Index Variation of Fe₃O₄ Thin Film According to Deposition Rate. in *Applied Mechanics and Materials: Trans Tech Publ.* pp. 106-110.
- Ji, Y., Strijkers, G., Yang, F., Chien, C., Byers, J., Anguelouch, A., Xiao, G. and Gupta, A. (2001) Determination of the spin polarization of half-metallic CrO₂ by point contact Andreev reflection. *Physical review letters*, 86(24), pp. 5585.

- Jia, C.-J., Sun, L.-D., Luo, F., Han, X.-D., Heyderman, L. J., Yan, Z.-G., Yan, C.-H., Zheng, K., Zhang, Z. and Takano, M. (2008) Large-scale synthesis of single-crystalline iron oxide magnetic nanorings. *Journal of the American Chemical Society*, 130(50), pp. 16968-16977.
- Jiang, C., Leung, C. W. and Pong, P. W. (2017) Self-assembled thin films of Fe₃O₄-Ag composite nanoparticles for spintronic applications. *Applied Surface Science*, 419, pp. 692-696.
- Jin, C., Mi, W., Li, P. and Bai, H. (2011) Experimental and first-principles study on the magnetic and transport properties of Ti-doped Fe₃O₄ epitaxial films. *Journal of applied physics*, 110(8), pp. 083905.
- Jin, C., Zhang, Q., Mi, W., Jiang, E. and Bai, H. (2010) Tunable magnetic and electrical properties of polycrystalline and epitaxial Ni_xFe_{3-x}O₄ thin films prepared by reactive co-sputtering. *Journal of Physics D: Applied Physics*, 43(38), pp. 385001.
- Joong Kim, K., Moon, D. W., Lee, S. K. and Jung, K.-H. (2000) Formation of a highly oriented FeO thin film by phase transition of Fe₃O₄ and Fe nanocrystallines. *Thin Solid Films*, 360(1), pp. 118-121.
- Joshi, V. K. (2016) Spintronics: A contemporary review of emerging electronics devices. *Engineering science and technology, an international journal*, 19(3), pp. 1503-1513.
- Julliere, M. (1975) Tunneling between ferromagnetic films. *Physics letters A*, 54(3), pp. 225-226.
- Jusman, Y., Ng, S. C., Osman, A. and Azuan, N. (2014) Investigation of CPD and HMDS sample preparation techniques for cervical cells in developing computer-aided screening system based on FE-SEM/EDX. *The scientific world journal*, 2014.
- Kale, S., Bhagat, S., Lofland, S., Scabarozzi, T., Ogale, S., Orozco, A., Shinde, S., Venkatesan, T., Hannoyer, B. and Mercey, B. (2001) Film thickness and temperature dependence of the magnetic properties of pulsed-laser-deposited Fe₃O₄ films on different substrates. *Physical Review B*, 64(20), pp. 205413.
- Kane, C. L. and Mele, E. J. (2005) Quantum spin Hall effect in graphene. *Physical review letters*, 95(22), pp. 226801.

- Karpan, V., Giovannetti, G., Khomyakov, P., Talanana, M., Starikov, A., Zwierzycki, M., Van Den Brink, J., Brocks, G. and Kelly, P. J. (2007) Graphite and graphene as perfect spin filters. *Physical review letters*, 99(17), pp. 176602.
- Kikkawa, J. and Awschalom, D. (1998) Resonant spin amplification in n-type GaAs. *Physical review letters*, 80(19), pp. 4313.
- Kikkawa, J. and Awschalom, D. (1999) Lateral drag of spin coherence in gallium arsenide. *nature*, 397(6715), pp. 139-141.
- Kikkawa, T., Suzuki, M., Ramos, R., Aguirre, M., Okabayashi, J., Uchida, K., Lucas, I., Anadón, A., Kikuchi, D. and Algarabel, P. A. (2019) Interfacial ferromagnetism and atomic structures in high-temperature grown Fe₃O₄/Pt/Fe₃O₄ epitaxial trilayers. *Journal of applied physics*, 126(14), pp. 143903.
- Kim, H.-J., Park, J.-H. and Vescovo, E. (2000a) Fe₃O₄ (111)/Fe (110) magnetic bilayer: Electronic and magnetic properties at the surface and interface. *Physical Review B*, 61(22), pp. 15288.
- Kim, H.-J., Park, J.-H. and Vescovo, E. (2000b) Oxidation of the Fe (110) surface: An Fe₃O₄ (111)/Fe (110) bilayer. *Physical Review B*, 61(22), pp. 15284.
- Kim, Y. K. and Oliveria, M. (1994) Magnetic properties of reactively sputtered Fe_{1-x}O and Fe₃O₄ thin films. *Journal of applied physics*, 75(1), pp. 431-437.
- Klewe, C., Meinert, M., Boehnke, A., Kuepper, K., Arenholz, E., Gupta, A., Schmalhorst, J.-M., Kuschel, T. and Reiss, G. (2014) Physical characteristics and cation distribution of NiFe₂O₄ thin films with high resistivity prepared by reactive co-sputtering. *Journal of applied physics*, 115(12), pp. 123903.
- Kodama, R. H., Berkowitz, A. E., McNiff Jr, E. and Foner, S. (1996) Surface spin disorder in NiFe₂O₄ nanoparticles. *Physical review letters*, 77(2), pp. 394.
- Koma, A. (1999) Van der Waals epitaxy for highly lattice-mismatched systems. *Journal of crystal growth*, 201, pp. 236-241.
- Koo, H. C., Kwon, J. H., Eom, J., Chang, J., Han, S. H. and Johnson, M. (2009) Control of spin precession in a spin-injected field effect transistor. *Science*, 325(5947), pp. 1515-1518.
- Kou, Z., Zhang, W., Wang, Y., Johnny Wong, P. K., Huang, H., Ji, C., Yue, J., Zhang, D., Zhai, Y. and Zhai, H. (2014) One-dimensional zinc ferrite nano-chains synthesis by chemical self-assembly assistant by magnetic field. *Journal of applied physics*, 115(17), pp. 17B524.

- Kronig, R. d. L. (1926) Spinning electrons and the structure of spectra. *nature*, *117*(2946), pp. 550-550.
- Kruglyak, V., Demokritov, S. and Grundler, D. (2010) Magnonics. *Journal of Physics D: Applied Physics*, *43*(26), pp. 264001.
- Kubaschewski, O. and Hopkins, B. E. (1962) *Oxidation of Metals and Alloys*, by O. Kubaschewski and B.E. Hopkins, Butterworths.
- Kumar, A., Pandya, D. K. and Chaudhary, S. (2012) Reduction in anti-ferromagnetic interactions in ion-beam deposited Fe₃O₄ thin films. *Journal of applied physics*, *111*(7), pp. 073901.
- Lai, C.-H., Huang, P.-H., Wang, Y.-J. and Huang, R. (2004) Room-temperature growth of epitaxial Fe₃O₄ films by ion beam deposition. *Journal of Applied Physics*, *95*(11), pp. 7222-7224.
- Lau, P. H., Takei, K., Wang, C., Ju, Y., Kim, J., Yu, Z., Takahashi, T., Cho, G. and Javey, A. (2013) Fully printed, high performance carbon nanotube thin-film transistors on flexible substrates. *Nano letters*, *13*(8), pp. 3864-3869.
- Lee, J.-M., Cho, D.-Y., Kim, Y., Noh, D., Park, B.-G., Kim, J.-Y. and Oh, S.-J. (2012) Characterization of Fe₃O₄/GaAs (100) ultrathin films prepared by oxidizing kinetically-stabilized Fe layers. *Thin Solid Films*, *526*, pp. 47-49.
- Lei, B., Han, S., Li, C., Zhang, D., Liu, Z. and Zhou, C. (2006) Synthesis and electronic properties of transition metal oxide core-shell nanowires. *Nanotechnology*, *18*(4), pp. 044019.
- Li, C., Van't Erve, O. and Jonker, B. (2011) Electrical injection and detection of spin accumulation in silicon at 500 K with magnetic metal/silicon dioxide contacts. *Nature communications*, *2*(1), pp. 1-7.
- Li, D., Zhou, X., Xu, Z., Man, J., Yuan, B., Liu, Y., Ortega, C. M., Sun, L. and Liu, Z. (2015) Electrodeposition of micro-nano size Fe₃O₄ crystals anchored on flexible buckypaper. *Journal of Solid State Electrochemistry*, *19*(10), pp. 3053-3058.
- Li, Y., Han, W., Swartz, A., Pi, K., Wong, J., Mack, S., Awschalom, D. and Kawakami, R. (2010) Oscillatory spin polarization and magneto-optical kerr effect in Fe₃O₄ thin films on GaAs (001). *Physical review letters*, *105*(16), pp. 167203.

- Liang, C., Huang, S., Zhao, W., Liu, W., Chen, J., Liu, H. and Tong, Y. (2015) Polyhedral Fe₃O₄ nanoparticles for lithium ion storage. *New Journal of Chemistry*, 39(4), pp. 2651-2656.
- Liao, Y., Li, Y., Hu, Z. and Chu, J. (2012) Temperature dependent phonon Raman scattering of highly a-axis oriented CoFe₂O₄ inverse spinel ferromagnetic films grown by pulsed laser deposition. *Applied Physics Letters*, 100(7), pp. 071905.
- Liao, Z.-M., Li, Y.-D., Xu, J., Zhang, J.-M., Xia, K. and Yu, D.-P. (2006) Spin-filter effect in magnetite nanowire. *Nano letters*, 6(6), pp. 1087-1091.
- Lin, M. S. and Leu, H. J. (2005) A Fe₃O₄-based chemical sensor for cathodic determination of hydrogen peroxide. *Electroanalysis: An International Journal Devoted to Fundamental and Practical Aspects of Electroanalysis*, 17(22), pp. 2068-2073.
- Lin, Y., Xu, H., Wang, Z., Cong, T., Liu, W., Ma, H. and Liu, Y. (2017) Transferable and flexible resistive switching memory devices based on PMMA films with embedded Fe₃O₄ nanoparticles. *Applied Physics Letters*, 110(19), pp. 193503.
- Liu, E., Zhang, J., Zhang, W., Wong, P., Lv, L., Zhai, Y., Wu, J., Xu, Y. and Zhai, H. (2011) Influence of Au capping layer on the magnetic properties of ultrathin epitaxial Fe₃O₄/GaAs (001) film. *Journal of applied physics*, 109(7), pp. 07C121.
- Liu, H.-J., Wang, C.-K., Su, D., Amrillah, T., Hsieh, Y.-H., Wu, K.-H., Chen, Y.-C., Juang, J.-Y., Eng, L. M. and Jen, S.-U. (2017) Flexible heteroepitaxy of CoFe₂O₄/Muscovite bimorph with large magnetostriction. *ACS applied materials & interfaces*, 9(8), pp. 7297-7304.
- Liu, H., Jiang, E., Bai, H. and Zheng, R. (2004a) Structure and magnetotransport properties of Fe₃O₄-SiO₂ composite films reactively sputtered at room temperature. *Journal of applied physics*, 95(10), pp. 5661-5665.
- Liu, H., Jiang, E., Bai, H., Zheng, R., Wei, H. and Zhang, X. (2003a) Large room-temperature spin-dependent tunneling magnetoresistance in polycrystalline Fe₃O₄ films. *Applied Physics Letters*, 83(17), pp. 3531-3533.
- Liu, H., Jiang, E., Bai, H., Zheng, R. and Zhang, X. (2003b) Thickness dependence of magnetic and magneto-transport properties of polycrystalline Fe₃O₄ films prepared by reactive sputtering at room temperature. *Journal of Physics D: Applied Physics*, 36(23), pp. 2950.

- Liu, H., Jiang, E., Zheng, R. and Bai, H. (2004b) Structure and magnetic properties of polycrystalline Fe_3O_4 films deposited by reactive sputtering at room temperature. *physica status solidi (a)*, 201(4), pp. 739-744.
- Liu, K., Zhao, L., Klavins, P., Osterloh, F. E. and Hiramatsu, H. (2003) Extrinsic magnetoresistance in magnetite nanoparticles. *Journal of applied physics*, 93(10), pp. 7951-7953.
- Liu, S.-J., Juang, J., Wu, K., Uen, T., Gou, Y. and Lin, J.-Y. (2002) Transport properties of CrO_2 (110) films grown on TiO_2 buffered Si substrates by chemical vapor deposition. *Applied Physics Letters*, 80(22), pp. 4202-4204.
- Liu, S., Tsai, H., Pao, C., Chiou, J., Ling, D., Pong, W., Tsai, M.-H., Lin, H., Jang, L. and Lee, J. (2006) Electronic and magnetic properties of the Ag-doped Fe_3O_4 films studied by x-ray absorption spectroscopy. *Applied Physics Letters*, 89(9), pp. 092112.
- Liu, W., Song, M., Maltby, N., Li, S., Lin, J., Samant, M., Parkin, S., Bencok, P., Steadman, P. and Dobrynin, A. (2015a) X-ray magnetic circular dichroism study of epitaxial magnetite ultrathin film on MgO (100). *Journal of applied physics*, 117(17), pp. 17E121.
- Liu, W., Wang, W., Wang, J., Wang, F., Lu, C., Jin, F., Zhang, A., Zhang, Q., Van Der Laan, G. and Xu, Y. (2015b) Atomic-scale interfacial magnetism in Fe/graphene heterojunction. *Scientific reports*, 5(1), pp. 1-9.
- Liu, W., Wong, P. K. J. and Xu, Y. (2019) Hybrid spintronic materials: Growth, structure and properties. *Progress in Materials Science*, 99, pp. 27-105.
- Liu, W., Xu, Y., Wong, P., Maltby, N., Li, S., Wang, X., Du, J., You, B., Wu, J. and Bencok, P. (2014) Spin and orbital moments of nanoscale Fe_3O_4 epitaxial thin film on MgO/GaAs (100). *Applied Physics Letters*, 104(14), pp. 142407.
- Liu, W., Zhou, Q., Chen, Q., Niu, D., Zhou, Y., Xu, Y., Zhang, R., Wang, J. and van der Laan, G. (2016) Probing the buried magnetic interfaces. *ACS applied materials & interfaces*, 8(9), pp. 5752-5757.
- Liu, X., Chang, C.-F., Rata, A. D., Komarek, A. C. and Tjeng, L. H. (2016) Fe_3O_4 thin films: controlling and manipulating an elusive quantum material. *npj Quantum Materials*, 1(1), pp. 1-5.
- Liu, X., Lu, H., He, M., Jin, K. and Yang, G. (2014a) Exchange bias in room-temperature epitaxial Fe_3O_4 film. *Solid state communications*, 188, pp. 23-26.

- Liu, X., Lu, H., He, M., Wang, L., Shi, H., Jin, K., Wang, C. and Yang, G. (2014b) Room-temperature layer-by-layer epitaxial growth and characteristics of Fe₃O₄ ultrathin films. *Journal of Physics D: Applied Physics*, 47(10), pp. 105004.
- Liu, X., Mi, W., Zhang, Q. and Zhang, X. (2017) Anisotropic magnetoresistance across Verwey transition in charge ordered Fe₃O₄ epitaxial films. *Physical Review B*, 96(21), pp. 214434.
- Liu, X., Rata, A., Chang, C., Komarek, A. and Tjeng, L. (2014) Verwey transition in Fe₃O₄ thin films: Influence of oxygen stoichiometry and substrate-induced microstructure. *Physical Review B*, 90(12), pp. 125142.
- Łodziana, Z. (2007) Surface Verwey transition in magnetite. *Physical review letters*, 99(20), pp. 206402.
- Lowndes, D. H., Geohegan, D., Puretzky, A., Norton, D. and Rouleau, C. (1996) Synthesis of novel thin-film materials by pulsed laser deposition. *Science*, 273(5277), pp. 898-903.
- Lu, A. H., Salabas, E. e. L. and Schüth, F. (2007) Magnetic nanoparticles: synthesis, protection, functionalization, and application. *Angewandte Chemie International Edition*, 46(8), pp. 1222-1244.
- Lu, Y., Claydon, J., Xu, Y., Schofield, D. and Thompson, S. (2004a) Magnetic properties of ultrathin Fe₃O₄ on GaAs (100). *Journal of applied physics*, 95(11), pp. 7228-7230.
- Lu, Y., Claydon, J., Xu, Y., Thompson, S., Wilson, K. and Van der Laan, G. (2004b) Epitaxial growth and magnetic properties of half-metallic Fe₃O₄ on GaAs (100). *Physical Review B*, 70(23), pp. 233304.
- Lu, Y., Yin, Y., Mayers, B. T. and Xia, Y. (2002) Modifying the surface properties of superparamagnetic iron oxide nanoparticles through a sol–gel approach. *Nano letters*, 2(3), pp. 183-186.
- Lu, Z., Xu, M., Zou, W., Wang, S., Liu, X., Lin, Y., Xu, J., Lu, Z., Wang, J. and Lv, L. (2007) Large low field magnetoresistance in ultrathin nanocrystalline magnetite Fe₃O₄ films at room temperature. *Applied Physics Letters*, 91(10), pp. 102508.
- Luysberg, M., Sofin, R., Arora, S. and Shvets, I. (2009) Strain relaxation in Fe₃O₄/MgAl₂O₄ heterostructures: Mechanism for formation of antiphase boundaries in an epitaxial system with identical symmetries of film and substrate. *Physical Review B*, 80(2), pp. 024111.

- Mantovan, R., Lamperti, A., Georgieva, M., Tallarida, G. and Fanciulli, M. (2010) CVD synthesis of polycrystalline magnetite thin films: structural, magnetic and magnetotransport properties. *Journal of Physics D: Applied Physics*, 43(6), pp. 065002.
- Margulies, D., Parker, F., Rudee, M., Spada, F., Chapman, J., Aitchison, P. and Berkowitz, A. (1997) Origin of the anomalous magnetic behavior in single crystal Fe₃O₄ films. *Physical review letters*, 79(25), pp. 5162.
- Margulies, D., Parker, F., Spada, F., Goldman, R., Li, J., Sinclair, R. and Berkowitz, A. (1996) Anomalous moment and anisotropy behavior in Fe₃O₄ films. *Physical Review B*, 53(14), pp. 9175.
- Master, R., Choudhary, R. and Phase, D. (2012) Effect of silver addition on structural, electrical and magnetic properties of Fe₃O₄ thin films prepared by pulsed laser deposition. *Journal of applied physics*, 111(7), pp. 073907.
- Master, R., Tiwari, S., Choudhary, R., Deshpande, U., Shripathi, T. and Phase, D. (2011) Infrared spectroscopic study of pulsed laser deposited Fe₃O₄ thin film on Si (111) substrate across Verwey transition temperature. *Journal of Applied Physics*, 109(4), pp. 043502-043502-3.
- Matsumoto, R., Takasaki, M., Tsukiyama, K., Oaki, Y. and Imai, H. (2018) Layer-by-Layer Manipulation of Heterogeneous Rectangular Nanoblocks: Brick Work for Multilayered Structures with Specific Heterojunction. *Inorganic chemistry*, 57(18), pp. 11655-11661.
- McCormack, M., Jin, S., Tiefel, T., Fleming, R., Phillips, J. M. and Ramesh, R. (1994) Very large magnetoresistance in perovskite-like La-Ca-Mn-O thin films. *Applied Physics Letters*, 64(22), pp. 3045-3047.
- McCray, W. P. (2007) MBE deserves a place in the history books. *Nature nanotechnology*, 2(5), pp. 259.
- McKenna, K. P., Hofer, F., Gilks, D., Lazarov, V. K., Chen, C., Wang, Z. and Ikuhara, Y. (2014) Atomic-scale structure and properties of highly stable antiphase boundary defects in Fe₃O₄. *Nature communications*, 5(1), pp. 1-8.
- Melzer, M., Makarov, D., Calvimontes, A., Karnaushenko, D., Baunack, S., Kaltofen, R., Mei, Y. and Schmidt, O. G. (2011) Stretchable magnetoelectronics. *Nano letters*, 11(6), pp. 2522-2526.

- Mi, W., Ye, T., Jiang, E. and Bai, H. (2010) Structure, magnetic and electrical transport properties of $(\text{Fe}_3\text{O}_4)_{100-x}\text{Pt}_x$ composite films. *Thin Solid Films*, 518(14), pp. 4035-4040.
- Mitra, A., Mohapatra, J., Meena, S., Tomy, C. and Aslam, M. (2014) Verwey transition in ultrasmall-sized octahedral Fe_3O_4 nanoparticles. *The Journal of Physical Chemistry C*, 118(33), pp. 19356-19362.
- Miyazaki, T. and Tezuka, N. (1995) Giant magnetic tunneling effect in $\text{Fe}/\text{Al}_2\text{O}_3/\text{Fe}$ junction. *Journal of Magnetism and Magnetic Materials*, 139(3), pp. L231-L234.
- Mohan Kant, K., Sethupathi, K. and Ramachandra Rao, M. (2008) Role of oxide barrier in intergranular tunnel junctions: An enhanced magnetoresistance in SiO_2 and ZnO coated Fe_3O_4 nanoparticle compacts. *Journal of applied physics*, 103(7), pp. 07F318.
- Monti, M., Sanz, M., Oujja, M., Rebollar, E., Castillejo, M., Pedrosa, F. J., Bollero, A., Camarero, J., Cunado, J. L. F. and Nemes, N. M. (2013) Room temperature in-plane $\langle 100 \rangle$ magnetic easy axis for $\text{Fe}_3\text{O}_4/\text{SrTiO}_3$ (001): Nb grown by infrared pulsed laser deposition. *Journal of Applied Physics*, 114(22), pp. 223902.
- Moodera, J. S., Kinder, L. R., Wong, T. M. and Meservey, R. (1995) Large magnetoresistance at room temperature in ferromagnetic thin film tunnel junctions. *Physical review letters*, 74(16), pp. 3273.
- Moore, G. E. (2006) Cramming more components onto integrated circuits, Reprinted from *Electronics*, volume 38, number 8, April 19, 1965, pp. 114 ff. *IEEE solid-state circuits society newsletter*, 11(3), pp. 33-35.
- Morel, A.-L., Nikitenko, S. I., Gionnet, K., Wattiaux, A., Lai-Kee-Him, J., Labrugere, C., Chevalier, B., Deleris, G., Petibois, C. and Brisson, A. (2008) Sonochemical approach to the synthesis of $\text{Fe}_3\text{O}_4@2$ core-shell nanoparticles with tunable properties. *ACS nano*, 2(5), pp. 847-856.
- Morrall, P., Schedin, F., Case, G., Thomas, M., Dudzik, E., Van der Laan, G. and Thornton, G. (2003) Stoichiometry of $\text{Fe}_{3-\delta}\text{O}_4$ (111) ultrathin films on Pt (111). *Physical Review B*, 67(21), pp. 214408.
- Moussy, J.-B. (2013) From epitaxial growth of ferrite thin films to spin-polarized tunnelling. *Journal of Physics D: Applied Physics*, 46(14), pp. 143001.

- Moussy, J.-B., Gota, S., Bataille, A., Guittet, M.-J., Gautier-Soyer, M., Delille, F., Dieny, B., Ott, F., Doan, T. and Warin, P. (2004) Thickness dependence of anomalous magnetic behavior in epitaxial Fe_3O_4 (111) thin films: Effect of density of antiphase boundaries. *Physical Review B*, 70(17), pp. 174448.
- Moyer, J., Vaz, C., Negusse, E., Arena, D. and Henrich, V. (2011) Controlling the electronic structure of $\text{Co}_{1-x}\text{Fe}_{2+x}\text{O}_4$ thin films through iron doping. *Physical Review B*, 83(3), pp. 035121.
- Nadgorny, B., Mazin, I., Osofsky, M., Soulen Jr, R., Broussard, P., Stroud, R., Singh, D., Harris, V., Arsenov, A. and Mukovskii, Y. (2001) Origin of high transport spin polarization in $\text{La}_{0.7}\text{Sr}_{0.3}\text{MnO}_3$: direct evidence for minority spin states. *Physical Review B*, 63(18), pp. 184433.
- Néel, M. L. (1948) Propriétés magnétiques des ferrites; ferrimagnétisme et antiferromagnétisme. in *Annales de physique*: EDP Sciences. pp. 137-198.
- Nielsen, A., Brandlmaier, A., Althammer, M., Kaiser, W., Opel, M., Simon, J., Mader, W., Goennenwein, S. and Gross, R. (2008) All oxide ferromagnet/semiconductor epitaxial heterostructures. *Applied Physics Letters*, 93(16), pp. 162510.
- Nurgaliev, T., Blagoev, B., Buchkov, K., Mateev, E., Gajda, G., Nedkov, I., Kovacheva, D., Slavov, L., Starbova, I., Starbov, N. and Nankovski, M. (2017) Magnetron sputtering of Fe-oxides on the top of HTS YBCO films. *Journal of Magnetism and Magnetic Materials*, 429, pp. 138-141.
- O'Handley, R. C. (1999) *Modern Magnetic Materials: Principles and Applications*, Wiley.
- O'handley, R. C. (2000) *Modern magnetic materials: principles and applications*, Wiley.
- Ogale, S., Ghosh, K., Sharma, R., Greene, R., Ramesh, R. and Venkatesan, T. (1998) Magnetotransport anisotropy effects in epitaxial magnetite (Fe_3O_4) thin films. *Physical Review B*, 57(13), pp. 7823.
- Omar, S. and van Wees, B. J. (2017) Graphene- WS_2 heterostructures for tunable spin injection and spin transport. *Physical Review B*, 95(8), pp. 081404.
- Opel, M. (2011) Spintronic oxides grown by laser-MBE. *Journal of Physics D: Applied Physics*, 45(3), pp. 033001.

- Orna, J., Algarabel, P., Morellón, L., Pardo, J., De Teresa, J., Antón, R. L., Bartolomé, F., García, L., Bartolomé, J. and Cezar, J. (2010) Origin of the giant magnetic moment in epitaxial Fe₃O₄ thin films. *Physical Review B*, 81(14), pp. 144420.
- Padilha, G. d. S., Giacon, V. M. and Bartoli, J. R. (2017) Effect of solvents on the morphology of PMMA films fabricated by spin-coating. *Polímeros*, 27(3), pp. 195-200.
- Palavesam, N., Marin, S., Hemmetzberger, D., Landesberger, C., Bock, K. and Kutter, C. (2018) Roll-to-roll processing of film substrates for hybrid integrated flexible electronics. *Flexible and Printed Electronics*, 3(1), pp. 014002.
- Pan, L., Zhang, G., Fan, C., Qiu, H., Wu, P., Wang, F. and Zhang, Y. (2005) Fabrication and characterization of Fe₃O₄ thin films deposited by reactive magnetron sputtering. *Thin Solid Films*, 473(1), pp. 63-67.
- Panja, S., Saha, B., Ghosh, S. and Chattopadhyay, S. (2013) Synthesis of novel four armed PE-PCL grafted superparamagnetic and biocompatible nanoparticles. *Langmuir*, 29(40), pp. 12530-12540.
- Paramês, M., Viskadourakis, Z., Rogalski, M., Mariano, J., Popovici, N., Giapintzakis, J. and Conde, O. (2007) Magnetic properties of Fe₃O₄ thin films grown on different substrates by laser ablation. *Applied Surface Science*, 253(19), pp. 8201-8205.
- Park, C., Peng, Y., Zhu, J.-G., Laughlin, D. E. and White, R. M. (2005a) Magnetoresistance of polycrystalline Fe₃O₄ films prepared by reactive sputtering at room temperature. *Journal of Applied Physics*, 97(10), pp. 10C303.
- Park, C., Zhu, J.-G., Peng, Y., Laughlin, D. E. and White, R. M. (2005b) Inverse magnetoresistance in magnetic tunnel junction with an Fe₃O₄ electrode. in *Magnetics Conference, 2005. INTERMAG Asia 2005. Digests of the IEEE International: IEEE*. pp. 2001-2008.
- Park, J.-H., Vescovo, E., Kim, H.-J., Kwon, C., Ramesh, R. and Venkatesan, T. (1998a) Direct evidence for a half-metallic ferromagnet. *nature*, 392(6678), pp. 794.
- Park, J.-H., Vescovo, E., Kim, H.-J., Kwon, C., Ramesh, R. and Venkatesan, T. (1998b) Magnetic properties at surface boundary of a half-metallic ferromagnet La_{0.7}Sr_{0.3}MnO₃. *Physical review letters*, 81(9), pp. 1953.

- Parkin, S. (1993) Origin of enhanced magnetoresistance of magnetic multilayers: Spin-dependent scattering from magnetic interface states. *Physical review letters*, 71(10), pp. 1641.
- Parkin, S., Bhadra, R. and Roche, K. (1991) Oscillatory magnetic exchange coupling through thin copper layers. *Physical review letters*, 66(16), pp. 2152.
- Parkin, S., More, N. and Roche, K. (1990) Oscillations in exchange coupling and magnetoresistance in metallic superlattice structures: Co/Ru, Co/Cr, and Fe/Cr. *Physical review letters*, 64(19), pp. 2304.
- Parkin, S. S. (1991) Systematic variation of the strength and oscillation period of indirect magnetic exchange coupling through the 3d, 4d, and 5d transition metals. *Physical review letters*, 67(25), pp. 3598.
- Parshin, A. M., Zyryanov, V. Y. and Shabanov, V. F. (2018) Structuring of the Surface Layer of Polycarbonate Film upon Interaction with Nematic Liquid Crystal. *Polymer Science, Series C*, 60(1), pp. 23-31.
- Pauli Jr, W. (1927) Zur Quantenmechanik des magnetischen Elektrons. *Zeitschrift für Physik*, 43(9-10), pp. 601-623.
- Peinado, P., Sangiao, S. and De Teresa, J. M. (2015) Focused electron and ion beam induced deposition on flexible and transparent polycarbonate substrates. *ACS nano*, 9(6), pp. 6139-6146.
- Peng, D., Asai, T., Nozawa, N., Hihara, T. and Sumiyama, K. (2002) Magnetic properties and magnetoresistance in small iron oxide cluster assemblies. *Applied Physics Letters*, 81(24), pp. 4598-4600.
- Peng, L., Chao, J., Wen-Bo, M. and Hai-Li, B. (2013) Reactively sputtered Fe₃O₄-based films for spintronics. *Chinese Physics B*, 22(4), pp. 047505.
- Peng, Y., Park, C. and Laughlin, D. E. (2003) Fe₃O₄ thin films sputter deposited from iron oxide targets. *Journal of applied physics*, 93(10), pp. 7957-7959.
- Pénicaud, M., Siberchicot, B., Sommers, C. and Kübler, J. (1992) Calculated electronic band structure and magnetic moments of ferrites. *Journal of Magnetism and Magnetic Materials*, 103(1-2), pp. 212-220.
- Pereira, C., Abbate, M., Schreiner, W., Boff, M., Teixeira, S. and Schmidt, J. (2000) Electronic structure of granular Fe–Al₂O₃ thin films prepared by co-evaporation. *Solid state communications*, 116(8), pp. 457-460.

- Petukhov, V. Y., Khabibullina, N., Ibragimova, M., Bukharaev, A., Biziaev, D., Zheglov, E., Gumarov, G. and Müller, R. (2007) Magnetic properties of thin metal-polymer films prepared by high-dose ion-beam implantation of iron and cobalt ions into polyethylene terephthalate. *Applied Magnetic Resonance*, 32(3), pp. 345-361.
- Pickett, W. E. and Moodera, J. S. (2001) Half metallic magnets. *Physics Today*, 54(5), pp. 39-45.
- Poddar, P., Fried, T. and Markovich, G. (2002) First-order metal-insulator transition and spin-polarized tunneling in Fe₃O₄ nanocrystals. *Physical Review B*, 65(17), pp. 172405.
- Poon, S., Pan, J. and Tok, E. (2006) Nucleation and growth of cobalt nanostructures on highly oriented pyrolytic graphite. *Physical Chemistry Chemical Physics*, 8(28), pp. 3326-3334.
- Powell, J. R. (2008) The quantum limit to Moore's law. *Proceedings of the IEEE*, 96(8), pp. 1247-1248.
- Prinz, G. A. (1998) Magnetoelectronics. *Science*, 282(5394), pp. 1660-1663.
- Pulido, B. A., Habboub, O. S., Aristizabal, S. L., Szekely, G. and Nunes, S. P. (2019) Recycled Poly(ethylene terephthalate) for High Temperature Solvent Resistant Membranes. *ACS Applied Polymer Materials*, 1(9), pp. 2379-2387.
- Ramos, A., Moussy, J.-B., Guittet, M.-J., Bataille, A., Gautier-Soyer, M., Viret, M., Gatel, C., Bayle-Guillemaud, P. and Snoeck, E. (2006) Magnetotransport properties of Fe₃O₄ epitaxial thin films: thickness effects driven by antiphase boundaries. *Journal of applied physics*, 100(10), pp. 103902.
- Ramos, R., Anadón, A., Lucas, I., Uchida, K., Algarabel, P., Morellón, L., Aguirre, M., Saitoh, E. and Ibarra, M. (2016) Thermoelectric performance of spin Seebeck effect in Fe₃O₄/Pt-based thin film heterostructures. *APL Materials*, 4(10), pp. 104802.
- Ramos, R., Arora, S. and Shvets, I. (2008) Anomalous anisotropic magnetoresistance in epitaxial Fe₃O₄ thin films on MgO (001). *Physical Review B*, 78(21), pp. 214402.
- Ramos, R., Kikkawa, T., Anadón, A., Lucas, I., Niizeki, T., Uchida, K., Algarabel, P. A., Morellón, L., Aguirre, M. and Ibarra, M. R. (2019) Interface-induced anomalous Nernst effect in Fe₃O₄/Pt-based heterostructures. *Applied Physics Letters*, 114(11), pp. 113902.

- Ramos, R., Kikkawa, T., Anadón, A., Lucas, I., Uchida, K., Algarabel, P. A., Morellón, L., Aguirre, M., Saitoh, E. and Ibarra, M. R. (2017) Temperature dependence of the spin Seebeck effect in [Fe₃O₄/Pt] n multilayers. *AIP Advances*, 7(5), pp. 055915.
- Ramos, R., Kikkawa, T., Uchida, K., Adachi, H., Lucas, I., Aguirre, M., Algarabel, P., Morellón, L., Maekawa, S. and Saitoh, E. (2013) Observation of the spin Seebeck effect in epitaxial Fe₃O₄ thin films. *Applied Physics Letters*, 102(7), pp. 072413.
- Ramos, R., Lucas, I., Algarabel, P. A., Morellón, L., Uchida, K., Saitoh, E. and Ibarra, M. R. (2018) Enhanced thermo-spin effects in iron-oxide/metal multilayers. *Journal of Physics D: Applied Physics*, 51(22), pp. 224003.
- Ran, F., Tsunemaru, Y., Hasegawa, T., Takeichi, Y., Harasawa, A., Yaji, K., Kim, S. and Kakizaki, A. (2011) Valence band structure and magnetic properties of Co-doped Fe₃O₄ (100) films. *Journal of applied physics*, 109(12), pp. 123919.
- Rashidian Vaziri, M., Hajiesmaeilbaigi, F. and Maleki, M. (2011) Monte Carlo simulation of the subsurface growth mode during pulsed laser deposition. *Journal of applied physics*, 110(4), pp. 043304.
- Ravindra, A., Padhan, P. and Prellier, W. (2012) Electronic structure and optical band gap of CoFe₂O₄ thin films. *Applied Physics Letters*, 101(16), pp. 161902.
- Ray, S. and Shard, A. G. (2011) Quantitative analysis of adsorbed proteins by X-ray photoelectron spectroscopy. *Analytical chemistry*, 83(22), pp. 8659-8666.
- Rubio-Zuazo, J., Onandia, L., Salas-Colera, E., Muñoz-Noval, A. and Castro, G. R. (2015) Incommensurate growth of thin and ultrathin films of single-phase Fe₃O₄ (001) on SrTiO₃ (001). *The Journal of Physical Chemistry C*, 119(2), pp. 1108-1112.
- Ruby, C., Humbert, B. and Fusy, J. (2000) Surface and interface properties of epitaxial iron oxide thin films deposited on MgO (001) studied by XPS and Raman spectroscopy. *Surface and Interface Analysis: An International Journal devoted to the development and application of techniques for the analysis of surfaces, interfaces and thin films*, 29(6), pp. 377-380.
- Rybchenko, S., Fujishiro, Y., Takagi, H. and Awano, M. (2005) Effect of grain boundaries on the magnetoresistance of magnetite. *Physical Review B*, 72(5), pp. 054424.

- Rybchenko, S., Fujishiro, Y., Takagi, H. and Awano, M. (2006) Effect of interface passivation on the magnetoresistance of granular magnetite $\text{Fe}_{3(1-\delta)}\text{O}_4$. *Applied Physics Letters*, 89(13), pp. 132509.
- Saito, H., Watanabe, S., Mineno, Y., Sharma, S., Jansen, R., Yuasa, S. and Ando, K. (2011) Electrical creation of spin accumulation in p-type germanium. *Solid state communications*, 151(17), pp. 1159-1161.
- Saito, T., Tezuka, N., Matsuura, M. and Sugimoto, S. (2013) Spin injection, transport, and detection at room temperature in a lateral spin transport device with $\text{Co}_2\text{FeAl}_{0.5}\text{Si}_{0.5}/\text{n-GaAs}$ schottky tunnel junctions. *Applied Physics Express*, 6(10), pp. 103006.
- Saito, T., Tezuka, N. and Sugimoto, S. (2011) Electrical Transport Properties and Spin Injection in $\text{Co}_2\text{FeAl}_{0.5}\text{Si}_{0.5}/\text{GaAs}$ Junctions. *IEEE transactions on magnetics*, 47(10), pp. 2447-2450.
- Sanz, M., López-Arias, M., Rebollar, E., De Nalda, R. and Castillejo, M. (2011) Laser ablation and deposition of wide bandgap semiconductors: Plasma and nanostructure of deposits diagnosis. *Journal of Nanoparticle Research*, 13(12), pp. 6621-6631.
- Sanz, M., Oujja, M., Rebollar, E., Marco, J. F., de la Figuera, J., Monti, M., Bollero, A., Camarero, J., Pedrosa, F. J. and García-Hernández, M. (2013) Stoichiometric magnetite grown by infrared nanosecond pulsed laser deposition. *Applied Surface Science*, 282, pp. 642-651.
- Sanz, M., Walczak, M., Oujja, M., Cuesta, A. and Castillejo, M. (2009) Nanosecond pulsed laser deposition of TiO_2 : nanostructure and morphology of deposits and plasma diagnosis. *Thin Solid Films*, 517(24), pp. 6546-6552.
- Schedin, F., Hill, E., Van der Laan, G. and Thornton, G. (2004a) Magnetic properties of stoichiometric and nonstoichiometric ultrathin Fe_3O_4 (111) films on Al_2O_3 (0001). *Journal of applied physics*, 96(2), pp. 1165-1169.
- Schedin, F., Leung, L., Muryn, C., Hill, E., Scholl, A. and Thornton, G. (2004b) Photoemission electron microscopy and atomic force microscopy of epitaxial iron oxide films on $\alpha\text{-Al}_2\text{O}_3$ (0001). *Journal of applied physics*, 95(11), pp. 7450-7452.
- Schmidt, G., Ferrand, D., Molenkamp, L., Filip, A. and Van Wees, B. (2000) Fundamental obstacle for electrical spin injection from a ferromagnetic metal into a diffusive semiconductor. *Physical Review B*, 62(8), pp. R4790.

- Schwertmann, U. and Cornell, R. M. (2007) The iron oxides. *Iron Oxides in the Laboratory*, pp. 5-18.
- Sedlačák, M. (2021) Polymer Processing and Surfaces. *Polymers*, 13(4), pp. 536.
- Seifikar, S., Calandro, B., Deeb, E., Sachet, E., Yang, J., Maria, J.-P., Bassiri-Gharb, N. and Schwartz, J. (2012) Structural and magnetic properties of biaxially textured NiFe₂O₄ thin films grown on c-plane sapphire. *Journal of applied physics*, 112(12), pp. 123910.
- Seki, M., Takahashi, M., Ohshima, T., Yamahara, H. and Tabata, H. (2013) High spin polarization at room temperature in Ge-substituted Fe₃O₄ epitaxial thin film grown under high oxygen pressure. *Applied Physics Letters*, 103(21), pp. 212404.
- Sena, S., Lindley, R., Blythe, H., Sauer, C., Al-Kafarji, M. and Gehring, G. (1997) Investigation of magnetite thin films produced by pulsed laser deposition. *Journal of Magnetism and Magnetic Materials*, 176(2-3), pp. 111-126.
- Senn, M. S., Wright, J. P. and Attfield, J. P. (2012) Charge order and three-site distortions in the Verwey structure of magnetite. *nature*, 481(7380), pp. 173.
- Serrano-Guisan, S., Wu, H.-C., Boothman, C., Abid, M., Chun, B., Shvets, I. and Schumacher, H. (2011) Thickness dependence of the effective damping in epitaxial Fe₃O₄/MgO thin films. *Journal of applied physics*, 109(1), pp. 013907.
- Serrate, D., De Teresa, J., Algarabel, P., Fernández-Pacheco, R., Galibert, J. and Ibarra, M. (2005) Grain-boundary magnetoresistance up to 42 T in cold-pressed Fe₃O₄ nanopowders. *Journal of applied physics*, 97(8), pp. 084317.
- Shan, J., Bougiatioti, P., Liang, L., Reiss, G., Kuschel, T. and Van Wees, B. (2017) Nonlocal magnon spin transport in NiFe₂O₄ thin films. *Applied Physics Letters*, 110(13), pp. 132406.
- Shan, J., Singh, A., Liang, L., Cornelissen, L., Galazka, Z., Gupta, A., van Wees, B. and Kuschel, T. (2018) Enhanced magnon spin transport in NiFe₂O₄ thin films on a lattice-matched substrate. *Applied Physics Letters*, 113(16), pp. 162403.
- Sheng, P. (1980) Fluctuation-induced tunneling conduction in disordered materials. *Physical Review B*, 21(6), pp. 2180.
- Sheng, P. (1992) Electronic transport in granular metal films. *Philosophical Magazine B*, 65(3), pp. 357-384.

- Sheng, P., Sichel, E. and Gittleman, J. (1978) Fluctuation-induced tunneling conduction in carbon-polyvinylchloride composites. *Physical review letters*, 40(18), pp. 1197.
- Shepherd, J., Koenitzer, J., Aragón, R., Spal, J. and Honig, J. (1991) Heat capacity and entropy of nonstoichiometric magnetite $\text{Fe}_{3(1-\delta)}\text{O}_4$: The thermodynamic nature of the Verwey transition. *Physical Review B*, 43(10), pp. 8461.
- Shi, S., Cao, L., Gao, H., Tian, Z., Bi, W., Geng, C. and Xu, S. (2021) Solvent- and initiator-free fabrication of efficient and stable perovskite-polystyrene surface-patterned thin films for LED backlights. *Nanoscale*, 13(20), pp. 9381-9390.
- Shim, S. H., Kim, H.-j., Koo, H. C., Lee, Y.-H. and Chang, J. (2015) Electrical spin injection in modulation-doped GaAs from an in situ grown Fe/MgO layer. *Applied Physics Letters*, 107(10), pp. 102407.
- Shklovskii, B. and Efros, A. (1984) Springer Series in Solid-State Sciences. in *Electronic properties of doped semiconductors*: Springer-Verlag Berlin. pp. 45.
- Sigmund, P. (1987) Mechanisms and theory of physical sputtering by particle impact. *Nuclear Instruments and Methods in Physics Research Section B: Beam Interactions with Materials and Atoms*, 27(1), pp. 1-20.
- Singh, L., Barber, Z., Kohn, A., Petford-Long, A., Miyoshi, Y., Bugoslavsky, Y. and Cohen, L. (2006) Interface effects in highly oriented films of the Heusler alloy Co_2MnSi on GaAs (001). *Journal of applied physics*, 99(1), pp. 013904.
- Singh, M., Chaudhary, S., Kashyap, S. C. and Pandya, D. (2011) Synthesis and Investigation of Electrodeposited Half-Metallic Fe_3O_4 Thin Films and Nanowires. *Journal of Superconductivity and Novel Magnetism*, 24(1-2), pp. 845-849.
- Singh, S. K., Husain, S., Kumar, A. and Chaudhary, S. (2018) Effect of oxygen partial pressure on the density of antiphase boundaries in Fe_3O_4 thin films on Si (100). *Journal of Magnetism and Magnetic Materials*, 448, pp. 303-309.
- Slonczewski, J. C. (1996) Current-driven excitation of magnetic multilayers. *Journal of Magnetism and Magnetic Materials*, 159(1-2), pp. L1-L7.
- Soares, E., Abreu, G., Carara, S., Paniago, R., De Carvalho, V. and Chacham, H. (2013) Graphene-protected Fe layers atop Ni (111): Evidence for strong Fe-graphene interaction and structural bistability. *Physical Review B*, 88(16), pp. 165410.

- Sofin, R., Arora, S. and Shvets, I. (2011) Positive antiphase boundary domain wall magnetoresistance in Fe₃O₄ (110) heteroepitaxial films. *Physical Review B*, 83(13), pp. 134436.
- Sokolov, A., Yang, C.-S., Yuan, L., Liou, S.-H., Cheng, R., Xu, B., Borca, C., Dowben, P. A. and Doudin, B. (2002) Spin blockade effects in chromium oxide intergrain magnetoresistance. *Journal of applied physics*, 91(10), pp. 8801-8803.
- Solís, C., Somacescu, S., Palafox, E., Balaguer, M. and Serra, J. M. (2014) Particular transport properties of NiFe₂O₄ thin films at high temperatures. *The Journal of Physical Chemistry C*, 118(42), pp. 24266-24273.
- Sorenson, T. A., Morton, S. A., Waddill, G. D. and Switzer, J. A. (2002) Epitaxial electrodeposition of Fe₃O₄ thin films on the low-index planes of gold. *Journal of the American Chemical Society*, 124(25), pp. 7604-7609.
- Soulen, R., Byers, J., Osofsky, M., Nadgorny, B., Ambrose, T., Cheng, S., Broussard, P. R., Tanaka, C., Nowak, J. and Moodera, J. (1998) Measuring the spin polarization of a metal with a superconducting point contact. *Science*, 282(5386), pp. 85-88.
- Stampe, P., Kennedy, R., Watts, S. and von Molnár, S. (2001) Strain effects in thin films of CrO₂ on rutile and sapphire substrates. *Journal of applied physics*, 89(11), pp. 7696-7698.
- Stern, O. (1921) Ein weg zur experimentellen prüfung der richtungsquantelung im magnetfeld. *Zeitschrift für Physik*, 7(1), pp. 249-253.
- Sugahara, S. and Tanaka, M. (2004) A spin metal–oxide–semiconductor field-effect transistor using half-metallic-ferromagnet contacts for the source and drain. *Applied Physics Letters*, 84(13), pp. 2307-2309.
- Sun, L., Ban, D., Liu, E., Li, X., Peng, H., Yao, Z., Huang, Z., Zhai, Y. and Zhai, H. (2020) Effect of substrate temperature on antiphase boundaries and spin polarization of thin Fe₃O₄ film on Si (100). *Thin Solid Films*, 693, pp. 137698.
- Sun, S., Zeng, H., Robinson, D. B., Raoux, S., Rice, P. M., Wang, S. X. and Li, G. (2004) Monodisperse MFe₂O₄ (M = Fe, Co, Mn) nanoparticles. *Journal of the American Chemical Society*, 126(1), pp. 273-279.
- Sun, X., Pratt, A. and Yamauchi, Y. (2010) First-principles study of the structural and magnetic properties of graphene on a Fe/Ni (1 1 1) surface. *Journal of Physics D: Applied Physics*, 43(38), pp. 385002.

- Sundar Manoharan, S., Elefant, D., Reiss, G. and Goodenough, J. (1998) Extrinsic giant magnetoresistance in chromium (IV) oxide, CrO₂. *Applied Physics Letters*, 72(8), pp. 984-986.
- Suzuki, K. and Tedrow, P. (1998) Resistivity and magnetotransport in CrO₂ films. *Physical Review B*, 58(17), pp. 11597.
- Suzuki, K. and Tedrow, P. (1999) Longitudinal magnetoresistance of CrO₂ thin films. *Applied Physics Letters*, 74(3), pp. 428-429.
- Takahashi, R., Cho, Y. and Lippmaa, M. (2015) Interfacial capacitance between a ferroelectric Fe₃O₄ thin film and a semiconducting Nb:SrTiO₃ substrate. *Journal of applied physics*, 117(1), pp. 014104.
- Takahashi, R., Misumi, H. and Lippmaa, M. (2014) Growth temperature effect on the structural and magnetic properties of Fe₃O₄ films grown by the self-template method. *Journal of applied physics*, 116(3), pp. 033918.
- Takahashi, S., Imamura, H. and Maekawa, S. (2006) Concepts in Spin Electronics. *Concepts in Spin Electronics*, Oxford University Press, UK, pp. 343-370.
- Takaobushi, J., Tanaka, H., Kawai, T., Ueda, S., Kim, J.-J., Kobata, M., Ikenaga, E., Yabashi, M., Kobayashi, K. and Nishino, Y. (2006) Fe_{3-x}Zn_xO₄ thin film as tunable high Curie temperature ferromagnetic semiconductor. *Applied Physics Letters*, 89(24), pp. 242507.
- Tang, J., Wang, K.-Y. and Zhou, W. (2001) Magnetic properties of nanocrystalline Fe₃O₄ films. *Journal of applied physics*, 89(11), pp. 7690-7692.
- Terris, B. and Thomson, T. (2005) Nanofabricated and self-assembled magnetic structures as data storage media. *Journal of Physics D: Applied Physics*, 38(12), pp. R199.
- Thompson, S. E. and Parthasarathy, S. (2006) Moore's law: the future of Si microelectronics. *Materials Today*, 9(6), pp. 20-25.
- Tian, H., Qu, T., Luo, L., Yang, J., Guo, S., Zhang, H., Zhao, Y. and Li, J. (2008) Strain induced magnetoelectric coupling between magnetite and BaTiO₃. *Applied Physics Letters*, 92(6), pp. 063507.
- Tiwari, S., Prakash, R., Choudhary, R. and Phase, D. (2007) Oriented growth of Fe₃O₄ thin film on crystalline and amorphous substrates by pulsed laser deposition. *Journal of Physics D: Applied Physics*, 40(16), pp. 4943.

- Tran, T. L. A., Wong, P. K. J., Jong, M. P. d., Wiel, W. G. v. d., Zhan, Y. Q. and Fahlman, M. (2011) Hybridization-induced oscillatory magnetic polarization of C60 orbitals at the C60/Fe(001) interface. *Applied Physics Letters*, 98(22), pp. 222505.
- Tripathy, D., Adeyeye, A., Boothroyd, C. and Shannigrahi, S. (2008) Microstructure and magnetotransport properties of Cu doped Fe₃O₄ films. *Journal of applied physics*, 103(7), pp. 07F701.
- Tsuchiya, T., Terabe, K., Ochi, M., Higuchi, T., Osada, M., Yamashita, Y., Ueda, S. and Aono, M. (2016) In situ tuning of magnetization and magnetoresistance in Fe₃O₄ thin film achieved with all-solid-state redox device. *ACS nano*, 10(1), pp. 1655-1661.
- Uchida, K., Iguchi, R., Daimon, S., Ramos, R., Anadón, A., Lucas, I., Algarabel, P. A., Morellón, L., Aguirre, M. H. and Ibarra, M. R. (2017) Enhancement of the spin Peltier effect in multilayers. *Physical Review B*, 95(18), pp. 184437.
- Uchida, K., Takahashi, S., Harii, K., Ieda, J., Koshibae, W., Ando, K., Maekawa, S. and Saitoh, E. (2008) Observation of the spin Seebeck effect. *nature*, 455(7214), pp. 778.
- Uhlenbeck, G. E. and Goudsmit, S. (1926) Spinning Electrons and the Structure of Spectra. *nature*, 117, pp. 264.
- Utama, M. I. B., de la Mata, M., Magen, C., Arbiol, J. and Xiong, Q. (2013) Twinning-, Polytypism-, and Polarity-Induced Morphological Modulation in Nonplanar Nanostructures with van der Waals Epitaxy. *Advanced Functional Materials*, 23(13), pp. 1636-1646.
- van Dijken, S., Fain, X., Watts, S. M. and Coey, J. (2004) Negative magnetoresistance in Fe₃O₄/Au/Fe spin valves. *Physical Review B*, 70(5), pp. 052409.
- Vanalakar, S., Agawane, G., Shin, S., Suryawanshi, M., Gurav, K., Jeon, K., Patil, P., Jeong, C., Kim, J. and Kim, J. (2015) A review on pulsed laser deposited CZTS thin films for solar cell applications. *Journal of Alloys and Compounds*, 619, pp. 109-121.
- Vázquez, M. (2007) Handbook of magnetism and advanced magnetic materials. *Novel materials*, 4, pp. 1-29.

- Vemulkar, T., Mansell, R., Fernández-Pacheco, A. and Cowburn, R. P. (2016) Toward flexible spintronics: perpendicularly magnetized synthetic antiferromagnetic thin films and nanowires on polyimide substrates. *Advanced Functional Materials*, 26(26), pp. 4704-4711.
- Venkatesan, M., Nawka, S., Pillai, S. and Coey, J. (2003) Enhanced magnetoresistance in nanocrystalline magnetite. *Journal of applied physics*, 93(10), pp. 8023-8025.
- Venkateshvaran, D., Althammer, M., Nielsen, A., Geprägs, S., Rao, M. R., Goennenwein, S. T., Opel, M. and Gross, R. (2009) Epitaxial $Zn_xFe_{3-x}O_4$ thin films: a spintronic material with tunable electrical and magnetic properties. *Physical Review B*, 79(13), pp. 134405.
- Verma, K. C., Singh, V. P., Ram, M., Shah, J. and Kotnala, R. (2011) Structural, microstructural and magnetic properties of $NiFe_2O_4$, $CoFe_2O_4$ and $MnFe_2O_4$ nanoferrite thin films. *Journal of Magnetism and Magnetic Materials*, 323(24), pp. 3271-3275.
- Versluijs, J., Bari, M. and Coey, J. (2001) Magnetoresistance of half-metallic oxide nanocontacts. *Physical review letters*, 87(2), pp. 026601.
- Verwey, E. (1939) Electronic conduction of magnetite (Fe_3O_4) and its transition point at low temperatures. *nature*, 144(3642), pp. 327.
- Verwey, E. and Haayman, P. (1941) Electronic conductivity and transition point of magnetite (“ Fe_3O_4 ”). *Physica*, 8(9), pp. 979-987.
- Vikulov, V., Balashev, V., Pisarenko, T., Dimitriev, A. and Korobtsov, V. (2012) The effect of synthesis temperature on structural and magnetic properties of Fe_3O_4 films grown on the SiO_2/Si (001) surface. *Technical Physics Letters*, 38(4), pp. 336-339.
- Volger, J. (1954) Further experimental investigations on some ferromagnetic oxidic compounds of manganese with perovskite structure. *Physica*, 20(1-6), pp. 49-66.
- von Helmolt, R., Wecker, J., Holzzapfel, B., Schultz, L. and Samwer, K. (1993) Giant negative magnetoresistance in perovskitelike $La_{2/3}Ba_{1/3}MnO_x$ ferromagnetic films. *Physical review letters*, 71(14), pp. 2331.
- Voogt, F., Fujii, T., Smulders, P., Niesen, L., James, M. and Hibma, T. (1999) NO_2 -assisted molecular-beam epitaxy of Fe_3O_4 , $Fe_{3-\delta}O_4$, and $\gamma-Fe_2O_3$ thin films on MgO (100). *Physical Review B*, 60(15), pp. 11193.

- Voogt, F., Palstra, T., Niesen, L., Rogojanu, O., James, M. and Hibma, T. (1998) Superparamagnetic behavior of structural domains in epitaxial ultrathin magnetite films. *Physical Review B*, 57(14), pp. R8107.
- Walz, F. (2002) The Verwey transition-a topical review. *Journal of Physics: Condensed Matter*, 14(12), pp. R285.
- Wang, J., Shi, W., Luo, Z., Chen, S. and Xue, K. (2020) Reversible polystyrene-block-poly (methyl methacrylate) copolymer films with perpendicular orientation by ultra-thin polystyrene substrates. *Progress in Organic Coatings*, 147, pp. 105721.
- Wang, L., Bao, J., Wang, L., Zhang, F. and Li, Y. (2006) One-pot synthesis and bioapplication of amine-functionalized magnetite nanoparticles and hollow nanospheres. *Chemistry–A European Journal*, 12(24), pp. 6341-6347.
- Wang, W., Liu, Y., Tang, L., Jin, Y., Zhao, T. and Xiu, F. (2014) Controllable Schottky barriers between MoS₂ and permalloy. *Scientific reports*, 4, pp. 6928.
- Wang, W., Narayan, A., Tang, L., Dolui, K., Liu, Y., Yuan, X., Jin, Y., Wu, Y., Rungger, I. and Sanvito, S. (2015) Spin-valve effect in NiFe/MoS₂/NiFe junctions. *Nano letters*, 15(8), pp. 5261-5267.
- Wang, W., Yu, M., Batzill, M., He, J., Diebold, U. and Tang, J. (2006a) Enhanced tunneling magnetoresistance and high-spin polarization at room temperature in a polystyrene-coated Fe₃O₄ granular system. *Physical Review B*, 73(13), pp. 134412.
- Wang, W., Yu, M., Chen, Y. and Tang, J. (2006b) Large room-temperature spin-dependent tunneling magnetoresistance in a Fe₃O₄-polymer composite system. *Journal of applied physics*, 99(8), pp. 08J108.
- Wang, X., Wang, C., Anderson, S. and Zhang, X. (2013) Characterization of reactively sputtered iron oxide thin films for developing magnetic resonance imaging contrast agents. in *2013 Transducers & Eurosensors XXVII: The 17th International Conference on Solid-State Sensors, Actuators and Microsystems (TRANSDUCERS & EUROSENSORS XXVII)*: IEEE. pp. 2403-2406.
- Watanabe, M. and Abe, S. (2016) Out-of-Plane Magnetic Moment and Lattice Distortion in Sputtered Ge Added Fe₃O₄ Thin Film. *Journal of nanoscience and nanotechnology*, 16(3), pp. 2509-2516.
- Watts, J. F. (1994) X-ray photoelectron spectroscopy. *Surface science techniques*, pp. 5-23.

- Watts, S. M., Wirth, S., Von Molnar, S., Barry, A. and Coey, J. (2000) Evidence for two-band magnetotransport in half-metallic chromium dioxide. *Physical Review B*, 61(14), pp. 9621.
- Weiss, W. and Ritter, M. (1999) Metal oxide heteroepitaxy: Stranski-Krastanov growth for iron oxides on Pt (111). *Physical Review B*, 59(7), pp. 5201.
- Wen, C., Li, J., Kitazawa, K., Aida, T., Honma, I., Komiyama, H. and Yamada, K. (1992) Electrical conductivity of a pure C60 single crystal. *Applied Physics Letters*, 61(18), pp. 2162-2163.
- Weser, M., Rehder, Y., Horn, K., Sicot, M., Fonin, M., Preobrajenski, A. B., Voloshina, E. N., Goering, E. and Dedkov, Y. S. (2010) Induced magnetism of carbon atoms at the graphene/Ni (111) interface. *Applied Physics Letters*, 96(1), pp. 012504.
- Weser, M., Voloshina, E., Horn, K. and Dedkov, Y. S. (2011) Electronic structure and magnetic properties of the graphene/Fe/Ni (111) intercalation-like system. *Physical Chemistry Chemical Physics*, 13(16), pp. 7534-7539.
- Williams, D. B. and Carter, C. B. (1996) The transmission electron microscope. in *Transmission electron microscopy*: Springer. pp. 3-17.
- Wolf, S., Awschalom, D., Buhrman, R., Daughton, J., Von Molnar, S., Roukes, M., Chtchelkanova, A. Y. and Treger, D. (2001a) Spintronics: a spin-based electronics vision for the future. *Science*, 294(5546), pp. 1488-1495.
- Wolf, S., Awschalom, D., Buhrman, R., Daughton, J., von Molnár, v. S., Roukes, M., Chtchelkanova, A. Y. and Treger, D. (2001b) Spintronics: a spin-based electronics vision for the future. *Science*, 294(5546), pp. 1488-1495.
- Wong, J. J., Swartz, A. G., Zheng, R., Han, W. and Kawakami, R. K. (2012) Electric field control of the Verwey transition and induced magnetoelectric effect in magnetite. *Physical Review B*, 86(6), pp. 060409.
- Wong, P., de Jong, M. P., Leonardus, L., Siekman, M. H. and van der Wiel, W. G. (2011) Growth mechanism and interface magnetic properties of Co nanostructures on graphite. *Physical Review B*, 84(5), pp. 054420.
- Wong, P., Fu, Y., Zhang, W., Zhai, Y., Xu, Y., Huang, Z., Xu, Y. and Zhai, H. (2008) Influence of capping layers on magnetic anisotropy in Fe/MgO/GaAs (100) ultrathin films. *IEEE Transactions on Magnetics*, 44(11), pp. 2907-2910.

- Wong, P., Zhang, W., Cui, X., Xu, Y., Wu, J., Tao, Z., Li, X., Xie, Z., Zhang, R. and Van Der Laan, G. (2010) Ultrathin Fe₃O₄ epitaxial films on wide bandgap GaN (0001). *Physical Review B*, 81(3), pp. 035419.
- Wong, P. J., van Geijn, E., Zhang, W., Starikov, A. A., Tran, T. L. A., Sanderink, J. G., Siekman, M. H., Brocks, G., Kelly, P. J. and van der Wiel, W. G. (2013a) Crystalline CoFeB/graphite interfaces for carbon spintronics fabricated by solid phase epitaxy. *Advanced Functional Materials*, 23(39), pp. 4933-4940.
- Wong, P. J., Zhang, W., van der Laan, G. and de Jong, M. P. (2016) Hybridization-induced charge rebalancing at the weakly interactive C60/Fe₃O₄ (001) spinterface. *Organic electronics*, 29, pp. 39-43.
- Wong, P. J., Zhang, W., Wang, K., van der Laan, G., Xu, Y., van der Wiel, W. G. and de Jong, M. P. (2013b) Electronic and magnetic structure of C60/Fe₃O₄ (001): a hybrid interface for organic spintronics. *Journal of Materials Chemistry C*, 1(6), pp. 1197-1202.
- Wong, P. K. J. (2009) *Fabrication and characterization of hybrid magnetic semiconductor materials and devices*. Unpublished, The University of York.
- Wong, P. K. J., Tran, T. L. A., Brinks, P., van der Wiel, W. G., Huijben, M. and de Jong, M. P. (2013) Highly ordered C60 films on epitaxial Fe/MgO (0 0 1) surfaces for organic spintronics. *Organic electronics*, 14(2), pp. 451-456.
- Wong, P. K. J., Zhang, W., Cui, X., Will, I., Xu, Y., Tao, Z., Li, X., Xie, Z. and Zhang, R. (2011a) Growth evolution and superparamagnetism of ultrathin Fe films grown on GaN (0001) surfaces. *physica status solidi (a)*, 208(10), pp. 2348-2351.
- Wong, P. K. J., Zhang, W. and Xu, Y. (2011b) Interface electrical properties of Fe₃O₄/MgO/GaAs (100) epitaxial spin contacts. *physica status solidi (a)*, 208(10), pp. 2344-2347.
- Wong, P. K. J., Zhang, W., Xu, Y., Hassan, S. and Thompson, S. M. (2008) Magnetic and Structural Properties of Fully Epitaxial Fe₃O₄/MgO/GaAs (100) for Spin Injection. *IEEE Transactions on Magnetics*, 44(11), pp. 2640-2642.
- Wright, J. P., Attfield, J. and Radaelli, P. (2001) Long range charge ordering in magnetite below the Verwey transition. *Physical review letters*, 87(26), pp. 266401.

- Wu, H.-C., Coileáin, C. Ó., Abid, M., Mauit, O., Syrlybekov, A., Khalid, A., Xu, H., Gatensby, R., Wang, J. J. and Liu, H. (2015) Spin-dependent transport properties of Fe₃O₄/MoS₂/Fe₃O₄ junctions. *Scientific reports*, 5, pp. 15984.
- Wu, H.-C., Mauit, O., Coileáin, C. Ó., Syrlybekov, A., Khalid, A., Mouti, A., Abid, M., Zhang, H.-Z., Abid, M. and Shvets, I. V. (2014) Magnetic and transport properties of epitaxial thin film MgFe₂O₄ grown on MgO (100) by molecular beam epitaxy. *Scientific reports*, 4, pp. 7012.
- Wu, P.-C., Chen, P.-F., Do, T. H., Hsieh, Y.-H., Ma, C.-H., Ha, T. D., Wu, K.-H., Wang, Y.-J., Li, H.-B. and Chen, Y.-C. (2016) Heteroepitaxy of Fe₃O₄/muscovite: A new perspective for flexible spintronics. *ACS applied materials & interfaces*, 8(49), pp. 33794-33801.
- Xiang, H., Shi, F., Rzchowski, M. S., Voyles, P. M. and Chang, Y. A. (2010) Epitaxial growth and magnetic properties of Fe₃O₄ films on TiN buffered Si (001), Si (110), and Si (111) substrates. *Applied Physics Letters*, 97(9), pp. 092508.
- Xie, S., Sterbinsky, G. E., Wessels, B. W. and Dravid, V. P. (2010) Defect and interfacial structure of heteroepitaxial Fe₃O₄/BaTiO₃ bilayers. *Microscopy and Microanalysis*, 16(3), pp. 300.
- Xu, C., Ohno, K., Ladmiral, V., Milkie, D. E., Kikkawa, J. M. and Composto, R. J. (2009) Simultaneous block copolymer and magnetic nanoparticle assembly in nanocomposite films. *Macromolecules*, 42(4), pp. 1219-1228.
- Xu, Y., Freeland, D., Tselepi, M. and Bland, J. (2000) Uniaxial magnetic anisotropy of epitaxial Fe films on InAs(100)-4×2 and GaAs(100)-4×2. *Journal of applied physics*, 87(9), pp. 6110-6112.
- Xu, Y., Hassan, S., Wong, P., Wu, J., Claydon, J., Lu, Y., Damsgaard, C. D., Hansen, J., Jacobsen, C. and Zhai, Y. (2008) Hybrid spintronic structures with magnetic oxides and Heusler alloys. *IEEE Transactions on Magnetism*, 44(11), pp. 2959-2965.
- Xu, Y., Kernohan, E., Freeland, D., Ercole, A., Tselepi, M. and Bland, J. (1998) Evolution of the ferromagnetic phase of ultrathin Fe films grown on GaAs(100)-4×6. *Physical Review B*, 58(2), pp. 890.
- Xu, Y. and Thompson, S. (2006) *Spintronic materials and technology*, CRC press.
- Xu, Y., Tselepi, M., Wu, J., Wang, S., Bland, J., Huttel, Y. and Van Der Laan, G. (2002) Interface magnetic properties of epitaxial Fe-InAs heterostructures. *IEEE Transactions on Magnetism*, 38(5), pp. 2652-2654.

- Yang, C., Wu, J. and Hou, Y. (2011) Fe₃O₄ nanostructures: synthesis, growth mechanism, properties and applications. *Chemical Communications*, 47(18), pp. 5130-5141.
- Yang, K., Kim, D. and Dho, J. (2011) Schottky barrier effect on the electrical properties of Fe₃O₄/ZnO and Fe₃O₄/Nb:SrTiO₃ heterostructures. *Journal of Physics D: Applied Physics*, 44(35), pp. 355301.
- Yin, J.-X., Liu, Z.-G., Wu, S.-F., Wang, W.-H., Kong, W.-D., Richard, P., Yan, L. and Ding, H. (2016) Unconventional magnetization of Fe₃O₄ thin film grown on amorphous SiO₂ substrate. *AIP Advances*, 6(6), pp. 065111.
- Yoon, K. S. and Hong, J. P. (2017) Temperature-dependent anisotropic magnetoresistance inversion behaviors in Fe₃O₄ films. *Journal of Magnetism and Magnetic Materials*, 423, pp. 7-11.
- Yoon, K. S., Koo, J. H., Do, Y. H., Kim, K. W., Kim, C. O. and Hong, J. P. (2005) Performance of Fe₃O₄/AlO_x/CoFe magnetic tunnel junctions based on half-metallic Fe₃O₄ electrodes. *Journal of Magnetism and Magnetic Materials*, 285(1-2), pp. 125-129.
- Yuan, H., Liu, E., Yin, Y., Zhang, W., Wong, P. J., Zheng, J.-G., Huang, Z., Ou, H., Zhai, Y. and Xu, Q. (2016) Enhancement of magnetic moment in Zn_xFe_{3-x}O₄ thin films with dilute Zn substitution. *Applied Physics Letters*, 108(23), pp. 232403.
- Yuan, L., Ovchencov, Y., Sokolov, A., Yang, C.-S., Doudin, B. and Liou, S. H. (2003) Magnetotransport properties of CrO₂ films down to single-grain sizes. *Journal of applied physics*, 93(10), pp. 6850-6852.
- Zaanen, J., Sawatzky, G. and Allen, J. (1985) Band gaps and electronic structure of transition-metal compounds. *Physical review letters*, 55(4), pp. 418.
- Zeng, H., Black, C., Sandstrom, R., Rice, P., Murray, C. and Sun, S. (2006) Magnetotransport of magnetite nanoparticle arrays. *Physical Review B*, 73(2), pp. 020402.
- Zeng, Y., Hao, R., Xing, B., Hou, Y. and Xu, Z. (2010) One-pot synthesis of Fe₃O₄ nanoprisms with controlled electrochemical properties. *Chemical Communications*, 46(22), pp. 3920-3922.
- Zhai, Y., Huang, Z., Fu, Y., Ni, C., Lu, Y., Xu, Y., Wu, J. and Zhai, H. (2007) Anisotropy of ultrathin epitaxial Fe₃O₄ films on GaAs (100). *Journal of applied physics*, 101(9), pp. 09D126.

- Zhai, Y., Sun, L., Huang, Z., Lu, Y., Li, G., Li, Q., Xu, Y., Wu, J. and Zhai, H. (2010) Thickness dependence of the molecular magnetic moment of single crystal Fe₃O₄ films on GaAs (100). *Journal of applied physics*, 107(9), pp. 09B110.
- Zhang, J., Liu, W., Zhang, M., Zhang, X., Niu, W., Gao, M., Wang, X., Du, J., Zhang, R. and Xu, Y. (2017) Oxygen pressure-tuned epitaxy and magnetic properties of magnetite thin films. *Journal of Magnetism and Magnetic Materials*, 432, pp. 472-476.
- Zhang, J., Shang, X., Ren, H., Chi, J., Fu, H., Dong, B., Liu, C. and Chai, Y. (2019) Modulation of inverse spinel Fe₃O₄ by phosphorus doping as an industrially promising electrocatalyst for hydrogen evolution. *Advanced Materials*, 31(52), pp. 1905107.
- Zhang, W., Wong, P., Zhang, D., Yuan, S., Huang, Z., Zhai, Y., Wu, J. and Xu, Y. (2014) Magnetic anisotropies in epitaxial Fe₃O₄/GaAs (100) patterned structures. *AIP Advances*, 4(10), pp. 107111.
- Zhang, W., Wong, P. K. J., Zhang, D., Yue, J., Kou, Z., van der Laan, G., Scholl, A., Zheng, J. G., Lu, Z. and Zhai, Y. (2017) XMCD and XMCD-PEEM Studies on Magnetic-Field-Assisted Self-Assembled 1D Nanochains of Spherical Ferrite Particles. *Advanced Functional Materials*, 27(29), pp. 1701265.
- Zhang, W., Zhang, J., Wong, P., Huang, Z., Sun, L., Liao, J., Zhai, Y., Xu, Y. and van der Laan, G. (2011) In-plane uniaxial magnetic anisotropy in epitaxial Fe₃O₄-based hybrid structures on GaAs (100). *Physical Review B*, 84(10), pp. 104451.
- Zhang, Y., Sun, T., Zhang, D., Shi, Z., Zhang, X., Li, C., Wang, L., Song, J. and Lin, Q. (2020) Enhanced photodegradability of PVC plastics film by codoping nano-graphite and TiO₂. *Polymer Degradation and Stability*, 181, pp. 109332.
- Zhang, Z. and Satpathy, S. (1991) Electron states, magnetism, and the Verwey transition in magnetite. *Physical Review B*, 44(24), pp. 13319.
- Zhao, C., Ma, Y., Shen, C. and Han, W. (2016) Electrodeposition of Fe₃O₄ thin film and its application as anode for lithium ion batteries. *Journal of nanoscience and nanotechnology*, 16(1), pp. 950-955.
- Zheng, W., Zheng, D., Wang, Y., Jin, C. and Bai, H. (2018) Uniaxial strain tuning of the Verwey transition in flexible Fe₃O₄/muscovite epitaxial heterostructures. *Applied Physics Letters*, 113(14), pp. 142403.

- Zheng, W. C., Zheng, D. X., Wang, Y. C., Li, D., Jin, C. and Bai, H. L. (2019) Flexible $\text{Fe}_3\text{O}_4/\text{BiFeO}_3$ multiferroic heterostructures with uniaxial strain control of exchange bias. *Journal of Magnetism and Magnetic Materials*, 481, pp. 227-233.
- Zhou, W., Wang, K.-Y., O'Connor, C. and Tang, J. (2001) Granular growth of Fe_3O_4 thin films and its antiphase boundaries prepared by pulsed laser deposition. *Journal of applied physics*, 89(11), pp. 7398-7400.
- Zhu, M. and Diao, G. (2011) Synthesis of porous Fe_3O_4 nanospheres and its application for the catalytic degradation of xylenol orange. *The Journal of Physical Chemistry C*, 115(39), pp. 18923-18934.
- Zhu, Q.-X., Zheng, M., Yang, M.-M., Zheng, R.-K., Wang, Y., Li, X.-M. and Shi, X. (2014) Interface correlated exchange bias effect in epitaxial Fe_3O_4 thin films grown on SrTiO_3 substrates. *Applied Physics Letters*, 105(24), pp. 241604.
- Zhu, Y., Fang, Y. and Kaskel, S. (2010) Folate-conjugated $\text{Fe}_3\text{O}_4@/\text{SiO}_2$ hollow mesoporous spheres for targeted anticancer drug delivery. *The Journal of Physical Chemistry C*, 114(39), pp. 16382-16388.
- Zhu, Y., Kockrick, E., Ikoma, T., Hanagata, N. and Kaskel, S. (2009) An efficient route to rattle-type $\text{Fe}_3\text{O}_4@/\text{SiO}_2$ hollow mesoporous spheres using colloidal carbon spheres templates. *Chemistry of Materials*, 21(12), pp. 2547-2553.
- Ziese, M. (2002) Extrinsic magnetotransport phenomena in ferromagnetic oxides. *Reports on Progress in Physics*, 65(2), pp. 143.
- Ziese, M. and Blythe, H. (2000) Magnetoresistance of magnetite. *Journal of Physics: Condensed Matter*, 12(1), pp. 13.
- Ziese, M., Köhler, U., Bollero, A., Höhne, R. and Esquinazi, P. (2005) Schottky barrier and spin polarization at the $\text{Fe}_3\text{O}_4\text{-Nb:SrTiO}_3$ interface. *Physical Review B*, 71(18), pp. 180406.
- Ziese, M. and Thornton, M. J. (2007) *Spin electronics*, Springer.
- Zorpette, G. (2001) The quest for the SPIN transistor. *IEEE spectrum*, 38(12), pp. 30-35.
- Zou, X., Wu, J., Wong, P., Xu, Y., Zhang, R., Zhai, Y., Bunce, C. and Chantrell, R. (2011) Damping in magnetization dynamics of single-crystal $\text{Fe}_3\text{O}_4/\text{GaN}$ thin films. *Journal of applied physics*, 109(7), pp. 07D341.
- Žutić, I., Fabian, J. and Sarma, S. D. (2004) Spintronics: Fundamentals and applications. *Reviews of modern physics*, 76(2), pp. 323.

LIST OF PUBLICATIONS

Journal with Impact Factor

1. **Ansari, M. S.**, Othman, M. H. D., Ansari, M. O., Ansari, S., Yusop, M. Z. M. (2020). Room temperature growth of half-metallic Fe₃O₄ thin films on polycarbonate by reactive sputtering: Heterostructures for flexible spintronics. *Journal of Alloys and Compounds*, 816, pp. 152532. **(Q1, IF: 5.316)**
2. **Ansari, M. S.**, Othman, M. H. D., Ansari, M. O., Ansari, S., Abdullah, H. (2020). Reactively sputtered half-metallic Fe₃O₄ thin films at room temperature on polymethyl methacrylate: A perspective for flexible spintronics. *Ceramics International*, 46(11), pp. 19302–19310. **(Q1, IF: 4.527)**
3. **Ansari, M. S.**, Othman, M. H. D., Ansari, M. O., Ansari, S., Abdullah, H., Harun, Z. (2020). Magnetite thin films grown on different flexible polymer substrates at room temperature: Role of antiphase boundaries in electrical and magnetic properties. *Journal of Alloys and Compounds*, 846, 156368. **(Q1, IF: 5.316)**
4. **Ansari, M. S.**, Othman, M. H. D., Ansari, M. O., Ansari, S., Sazali, N. (2021). Large spin-dependent tunneling magnetoresistance in Fe₃O₄/PET heterostructures developed at room temperature: A promising candidate for flexible spintronics. *Materials Science & Engineering B*, 265, 115033. **(Q1, IF: 4.051)**
5. **Ansari, M. S.**, Othman, M. H. D., Ansari, M. O., Ansari, S., Abdullah, H. Progress in Fe₃O₄-centered spintronic systems: Development, architecture, and features, *Applied Materials Today* (Under review). **(Q1, IF: 10.041, Q1)**